Hindawi Publishing Corporation
ISRN Materials Science
Volume 2013, Article ID 302408, 24 pages
http://dx.doi.org/10.1155/2013/302408

Review Article

A Review of Neutron Scattering Applications to Nuclear Materials

Sven C. Vogel

Los Alamos Neutron Science Center, MS H805, Los Alamos National Laboratory, Los Alamos, NM 87545, USA

Correspondence should be addressed to Sven C. Vogel; sven@lanl.gov

Received 20 March 2013; Accepted 14 April 2013

Academic Editors: P. Karjalainen, A. O. Neto, E. Ntsoenzok, D. Sands, H. Saxén, and Y. Sun

The growing demand for electric energy will require expansion of the amount of nuclear power production in many countries of the world. Research and development in this field will continue to grow to further increase safety and efficiency of nuclear power generation. Neutrons are a unique probe for a wide range of problems related to these efforts, ranging from crystal chemistry of nuclear fuels to engineering diffraction on cladding or structural materials used in nuclear reactors. Increased flux at modern neutron sources combined with advanced sample environments allows nowadays, for example, studies of reaction kinetics at operating temperatures in a nuclear reactor. Neutrons provide unique data to benchmark simulations and modeling of crystal structure evolution and thermomechanical treatment. Advances in neutron detection recently opened up new avenues of materials characterization using neutron imaging with unparalleled opportunities especially for nuclear materials, where heavy elements (e.g., uranium) need to be imaged together with light elements (e.g., hydrogen, oxygen). This paper summarizes applications of neutron scattering techniques for nuclear materials. Directions for future research, extending the trends observed over the past decade, are discussed.

1. Introduction

Nuclear power accounts for approximately 13% of all electric power generated in the world and about 20% of the electric power in the United States [1]. For example, the United States alone have 104 operating nuclear power plants in 2012 spread over 31 states, with 35 of these reactors being boiling water reactors (BWRs) and the remaining 69 being pressurized water reactors (PWRs) [2]. Figure 1 shows the fraction of nuclear energy of the total energy production for selected countries.

Based on the fact that populations and energy demand in many of these countries will continue to grow, it is expected that the ratio of nuclear energy used to produce electricity will continue to grow, in particular in countries like India or China. The need to improve the efficiency and safety of power reactors is therefore of paramount importance from a global perspective. Some of the design features and operation goals of the so-called third-generation reactors are [3]

(i) a simpler and more rugged design, making them easier to operate and less vulnerable to operational upsets;

(ii) higher availability and longer operating life, typically 60 years;

(iii) further reduced possibility of core melt accidents;

(iv) resistance to serious damage that would allow radiological release from, for example, an aircraft impact or earthquake;

(v) higher burn-up to use fuel more fully and efficiently and reduce the amount of waste;

(vi) greater use of burnable absorbers ("poisons") to extend fuel life.

These goals require understanding and development of predictive models for changes in chemistry (e.g., phases, isotopes) and microstructure (grain sizes, texture) during operation and accident scenarios. These changes are the result of a complex interplay of irradiation, temperature, and mechanical and chemical effects, and even some of the single parameter variations, for example, temperature or stress only, are still not understood for all involved materials to the point where predictions over the anticipated life time of a reactor are reliable. Furthermore, new materials are

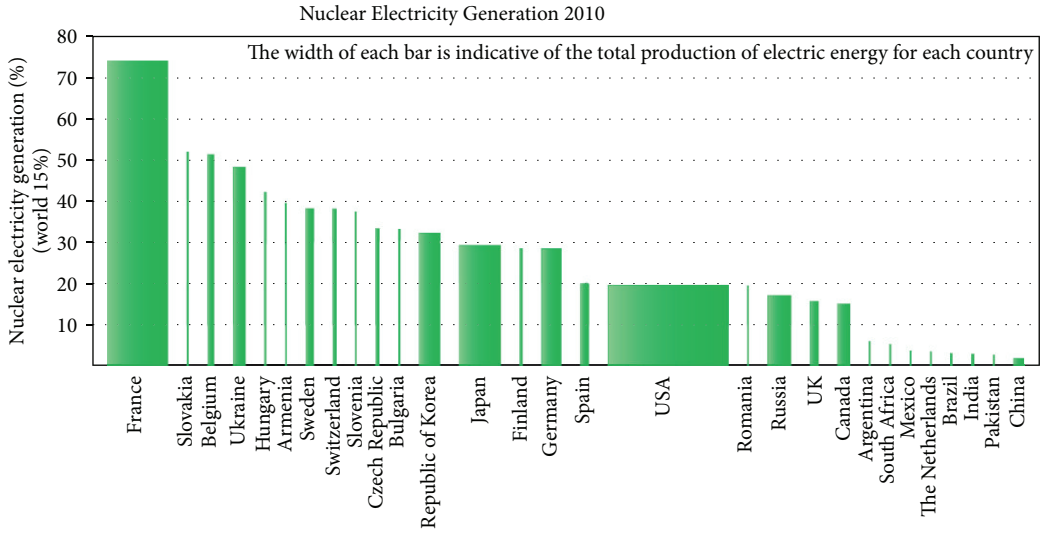

Figure 1: Fraction of electricity generated by nuclear power per country relative to the total electricity production of each country [1] (reproduced with permission).

introduced or are researched for optimization, for example, coatings for advanced cladding materials to prevent oxidation of the zirconium-based alloys used for the cladding or the aforementioned burnable absorbers. These newly introduced materials require not only characterization of their performance at operation and accident conditions, but also an understanding of their interaction with the existing materials under operation or accident scenarios. Techniques allowing to characterize materials in situ, that is, at operation or accident conditions, such as high temperatures or oxidizing atmospheres, without the need to rely on, for example, quenching for room temperature characterization, provide unique insight into the performance of materials and experimental data required for safety calculations. Furthermore, characterization of irradiated materials, that is, after a simulated service life, is challenging and nowadays frequently based on expensive destructive examination techniques. Developing advanced nondestructive characterization techniques for postirradiation examination (PIE), which can guide the destructive examination, has a great potential to accelerate the development and licensing of, for example, nuclear fuels.

Neutron scattering techniques, such as neutron diffraction or neutron radiography, evolved over more than four decades at user facilities [4] and have unique advantages for characterization of nuclear materials:

(i) Neutrons penetrate many materials to depths of several centimeters, hence allowing to use shielding or preventing the removal of the cladding material for characterization of, for example, irradiated fuels. X-rays or electrons are unable to penetrate, for example, a centimeter of Pb shielding.

(ii) Neutrons interact with the nuclei of the atoms, an interaction which is isotope specific. This allows for instance to study hydrogen distributions in components or both the uranium and oxygen sublattices in uranium-dioxide, whereas X-ray or electron diffraction would be heavily biased towards the heavier atoms.

(iii) Neutron beam-spot sizes are typically several cm^2, allowing to characterize larger objects with radiography or perform, for example, diffraction on materials which have experienced grain growth.

Neutrons uniquely complement other characterization techniques and together with synchrotrons, neutron facilities are considered the most useful microscopic probes of matter available today [5].

In this paper, we review how neutron scattering has been utilized in the past to nuclear materials, with a focus on the past decade but also mentioning ground-breaking older work. We also highlight recent developments in instrumentation, for example, beam lines, sample environments, or detectors, which enable new avenues of research in the future. Furthermore, we illustrate how neutron scattering may complement other advanced techniques, such as proton radiography. As the author has been working at the Los Alamos Neutron Science Center for the past decade, some focus is given to work at this facility but with the attempt to avoid a substantial bias. It is hoped that this paper may serve as an introduction for practitioners in nuclear engineering and related fields to neutron scattering techniques, ultimately leading to increased use of this marvelous technique in this field.

The outline of this paper is as follows: we review available neutron scattering user facilities in Section 2, including comments on their use for nuclear materials. Fundamentals of neutron diffraction and its application to fuels, cladding and structural materials are given in Section 3, including recent developments and an outlook. Neutron radiography is introduced in Section 4, again illustrating examples from fuels, cladding, and structural materials as well as recent developments and outlook. Other neutron scattering

techniques, such as cross-section measurements or inelastic scattering, are covered in Section 5. Section 6 summarizes this paper.

2. Neutron Scattering Facilities

Free neutrons have a half-life of 887.6 ± 3 seconds [6] and have to be produced shortly before the use in an experiment. For research, neutrons are produced in nuclear reactors or with spallation sources. The details of neutron production, moderation, beam optics, instrumentation, and detection are described in more detail elsewhere (e.g., [7–11]), and here we only give an overview of available neutron user facilities. The relevant instruments of concern for investigations of materials relevant to nuclear power generation are general purpose powder neutron diffractometers (phase analysis, in situ studies, etc.), engineering diffractometers (stress/strain measurements, deformation studies, etc.), small angle scattering machines (particle size and shape), and radiography stations (imaging, tomography). Most of the user facilities mentioned below have at least one instrument of each of these types. In general, instrument scientists at these facilities will gladly discuss new experiments with potential users. Special consideration has to be given to the ability to handle radioactive materials, especially powders, in case irradiated materials or inherently radioactive materials are to be characterized. Neutron facilities are better prepared for such materials as many samples are activated in the neutron beam, whereas such activation is not an issue, for example, at synchrotron user facilities, and consequently an infrastructure to handle radioactive materials is less prevalent. Research on nuclear materials is an active field of neutron applications, and for instance in the United States workshops are organized to bring potential users and facilities together [12].

The largest research reactor in the world is located at the Institut Laue-Langevin in Grenoble, France [13]. Modern research reactor facilities are also available in Australia with the OPAL reactor operated by the Australian Nuclear Science and Technology Organization ANSTO [14, 15], in Chalk River, Canada, where the NRU reactor [16, 17] is closely tied to the development of the CANDU power reactors, Germany's FRM-2 reactor at the Technical University Munich [18], the high-flux isotope reactor HFIR at Oak Ridge National Laboratory in the United States [19, 20], and the NIST Center for Neutron Research at Gaithersburg [21, 22], also in the United States. Several smaller reactors are available for research around the world [23]. All neutron reactors produce continuous polychromatic neutron beams, with the exception of the pulsed reactor at the Frank Laboratory of Neutron Physics, Joint Institute of Nuclear Research, Dubna, Russia [24, 25].

Due to reactor safety considerations, spallation sources are the neutron sources of choice to increase the neutron flux. Typically, these sources are operated in pulsed mode with the continuous spallation neutron source at the Paul Scherrer Institut (PSI) at the Swiss Spallation Neutron Source in Villigen, Switzerland [26, 27], being the exception. The Los Alamos Neutron Science Center LANSCE at Los Alamos National Laboratory [28, 29] and the ISIS source at the Rutherford Appleton Laboratory near Oxford in the United Kingdom [30, 31] have served the community as spallation neutron sources for several decades and both have ongoing instrument upgrades. The most recent neutron spallation sources are the Spallation Neutron Source SNS at Oak Ridge National Laboratory in the United States [32, 33] and the Japan Proton Accelerator Research Complex (J-PARC), Tokai, Japan [34, 35]. Planned spallation neutron sources include the European Spallation Source (ESS) planned to be built in Lund, Sweden [36], and the China Spallation Neutron Source (CSNS), Dongguan, Guangdong, China [37, 38].

3. Neutron Diffraction

3.1. Introduction. In this section we describe several applications of neutrons to investigate the crystallography and phase composition of nuclear materials, in particular fuels. Metallic uranium has an orthorhombic crystal structure, leading to anisotropic single crystal properties such as a negative thermal expansion along the crystallographic *b*-axis. This leads to substantial integrity problems when the material is heated. Besides the difficulties from the mechanical behavior, uranium melts at a comparably low temperature of 1132°C. Therefore, the vast majority of nuclear fuels in power reactors consist of cubic uranium dioxide (urania, UO_2), whereas in research reactors metallic fuels such as U_3Si dispersed in an aluminum matrix or uranium-molybdenum alloys are used, with molybdenum stabilizing the cubic γ-structure. During operation, that is, during heating and irradiation, atoms rearrange and phase transformations may occur, with the phases in a spent fuel having different material properties as those of a fresh fuel. The identification of the new phases, determination of their formation conditions and kinetics as well as establishing their properties, is of paramount importance for new and existing fuel types. Thermal gradients of several hundred degrees exist between the center and outside of a fuel rod, leading to a spatial distribution of crystallographic phases over a distance of the order of a centimeter. Similar considerations apply to structural materials, for example, the cladding or pressure tubing materials, and actinide-bearing minerals for mining, waste deposition, and accident scenarios [39].

In particular, for fuels the elements under consideration are high Z-number elements (uranium and other actinides) and low Z-number elements (oxygen, nitrogen, and carbon). For crystallographic investigations, neutron and X-ray diffraction fundamentally differ in the scattering power of individual atoms: The scattering power scales with the Z-number for X-rays, whereas for neutrons the scattering power depends on the isotope, but in a noncontinuous fashion and not as a function of Z. This leads to a heavy bias of the diffraction results towards the heavy atoms in the case of X-rays. As an example, Figure 2 shows simulated patterns for the three structure models proposed for cubic UC_2 [40–42], a nonquenchable phase existing between 1823 and 2104°C [43]. The three crystal structures are fundamentally different in the arrangement of the carbon atoms; however,

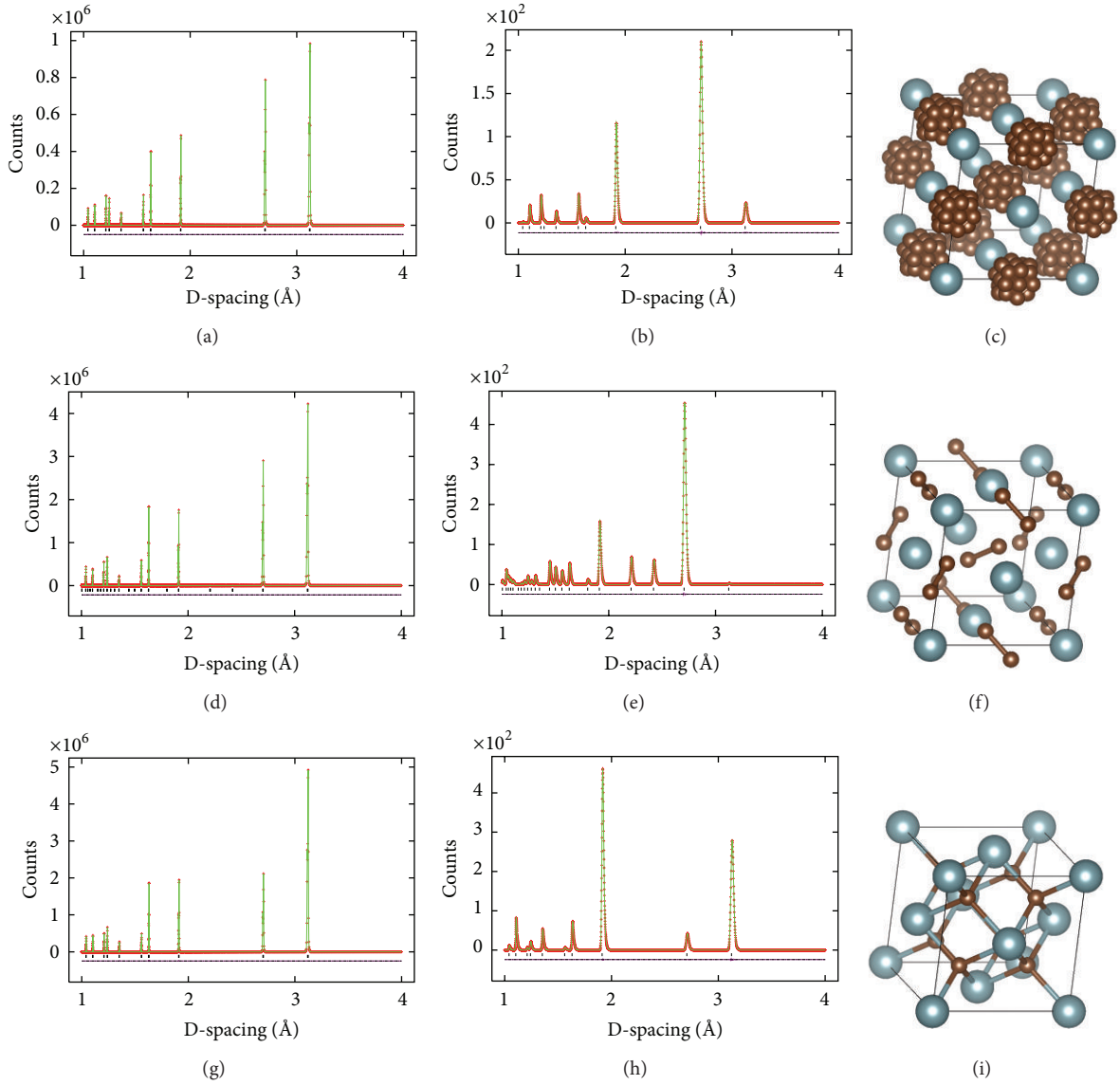

Figure 2: Simulated diffraction patterns for X-rays (a, d, g) and neutrons (b, e, h) of the three structures for the cubic high-temperature UC_2 phase proposed by Bowman et al. (a, b, c) [40], Bredig (d, e, f) [41], and Wilson (g, h, i) [42]. While the three proposed structures are substantially different, the X-ray diffraction patterns look very similar due to the bias of the diffraction signal to the uranium sublattice, virtually ignoring the carbon atoms. The neutron diffraction patterns, however, show distinct differences, allowing to unambiguously determine which of the proposed structures is present. The structure proposed by Bowman et al. [40] from neutron diffraction data suggests C-C dumbbells freely rotating, which is symbolized here by a cluster of carbon atoms. The structure by Bredig, determined from X-ray diffraction data, also suggests C-C dumbbells, but in a static position, resulting in a pyrite structure type. The structure proposed by Wilson, also based on X-ray diffraction data, is similar to the fluorite structure observed for UO_2. The diffraction data for X-rays is simulated for $Cu_K\alpha$ radiation ($\lambda = 1.5405$ Å), while the neutron diffraction data are simulated for the 90° bank of the HIPPO neutron time-of-flight diffractometer (see Figure 4) at LANSCE [77, 78]. Diffraction pattern simulations were performed using GSAS [204] and gsaslanguage [205]. Structure plots were produced with VESTA [206].

the simulated X-ray diffraction patterns appear very similar due to the bias towards the uranium sublattice, which is a face-centered cubic lattice in all three cases. The simulated neutron diffraction patterns on the other hand show the substantial contribution of the carbon sub-lattice to the diffraction signal, allowing to unambiguously discriminate the three different structures. This example illustrates the great advantages neutron diffraction offers over X-ray diffraction for crystal structure investigations of nuclear materials and in particular nuclear fuels. The crystal structure of UC_2 was also recently modeled using density functional theory (DFT) [44], confirming that the structure proposed by Bowman et al. based on neutron diffraction data is the correct structure. The DFT simulation also allows studying

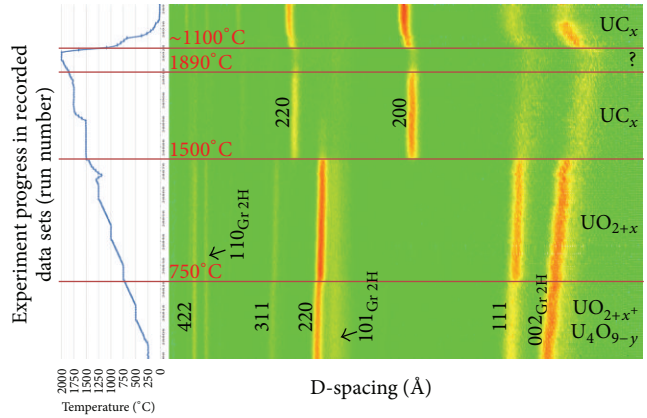

Figure 3: Overview of the diffraction data obtained in a neutron diffraction experiment on the HIPPO diffractometer to experimentally verify which of the three proposed structures for the high temperature cubic phase of UC_2 is experimentally observed. The three proposed structures are discussed in Figure 2. In this experiment, uranium carbide was synthesized in situ in a furnace from a mix of UO_2 and graphite powders. The experiment in the overview plot proceeds from bottom to top with the sample temperature shown on the left. UO_2 peaks are observed in the beginning, with the first transition to more intense diffraction peaks without changing the location of the peaks observed at ~750°C. At this temperature the two low-temperature urania phases UO_2 and $U_4O_{9-\delta}$ become a single UO_{2+x} hyperstoichiometric phase. At ~1500°C, the urania and graphite powders react to form UC_x. At ~1890°C the transition to the cubic UC_2 phase is observed. The substantial weakening of the diffraction signal is recovered upon cooling and results from the rotational disorder of the dumbbells discussed in Figure 2 (so-called sublattice melting). Detailed analysis of the data allowed to unambiguously confirm the structure determined by Bowman et al. [40] and predicted by Wen et al. [44]. See [207] for more details on these experiments.

the disorder of the C-C dumbbells in detail, which advanced data analysis techniques allow to verify experimentally with neutron diffraction. Again, neutron diffraction is a unique tool to provide experimental data for such structural investigations. Figure 3 provides an overview of the experimental data collected during an experiment aimed at resolving the conflicting three structure models for the cubic UC_2 phase. In this experiment, the uranium carbide was synthesized in situ from urania and graphite powders. As an example of a modern neutron powder diffractometer, Figure 4 shows the layout of the HIPPO instrument at LANSCE where these experiments were performed.

3.2. Fuel

3.2.1. Ceramic Fuels. As illustrated with the example of the cubic UC_2 phase, determination of the positions of light elements in the presence of heavier ones is a domain of neutron diffraction. In particular the complex crystallography of urania, which can accommodate a large range of hyperstoichiometric oxygen atoms, has been investigated by means of neutron diffraction. While stoichiometric UO_2 crystallizes in the CaF_2 structure, concentrations up to $UO_{2.25}$ are possible at elevated temperatures with the location of the excess oxygen atoms affecting lattice dynamics and therefore critical properties such as thermal expansion or thermal conductivity. At lower temperatures, several distinct crystallographic phases occur in the U-O phase diagram, many of which were determined and refined by neutron diffraction. As examples, Willis [45] utilized neutron diffraction from a $UO_{2.13}$ single crystal to establish the positions of the excess oxygen atoms in the CaF_2-type structure; neutron powder diffraction was used by Andresen to solve the crystal structure of U_3O_8 [46], pointing out problems with previous assessments using X-rays, and later refined by Loopstra also using neutron powder diffraction, but with a better resolution [47]; the crystal structure of β-U_4O_{9-y} was solved by Bevan et al. [48] and later refined by Cooper and Willis [49] using neutrons. Loopstra et al. [50] studied the phase evolution in UO_3 between 373 K and 77 K using neutron powder diffraction and remarkably found three different phases in this relatively small temperature range. The importance of neutron diffraction for investigations of urania is further illustrated by entries in the Inorganic Crystal Structure Database (ICSD, [51]) (Retrieved March 15, 2013): of 66 experimental structure records for urania UO_{2+x}, 55% (36 records) results from neutron diffraction work with the remainder being X-ray diffraction work. For all structures in the ICSD, the contribution of neutron diffraction work is only 16%.

Recent improvements in neutron flux allow studies of reaction kinetics in situ. This is relevant as, besides the equilibrium state, the rate at which a reaction occurs and the intermediate metastable phases are of practical importance. The sensitivity of neutron diffraction to the crystallographic phase is again of great importance here as dilatometry, gravimetry, and calorimetry are insensitive to the crystallographic phase but are sensitive to factors such as the amount of excess oxygen in the CaF_2-structure and phase transitions, complicating the interpretation of the data from these classical methods. As an example of kinetics studies, Higgs et al. [52] cycled a sample of hyperstoichiometric UO_{2+x} through the phase boundary between the low-temperature two-phase field and the high-temperature single-phase field with information of the concomitant oxygen redistribution derived from the lattice parameters. Such experimental data contributes to,

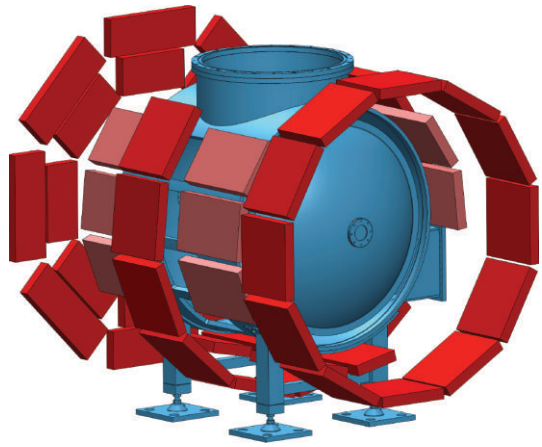

Figure 4: Schematic of the HIPPO general purpose neutron time-of-flight diffractometer at LANSCE [77, 78]. The red areas in the schematic are the 53 detectors panels, arranged on five rings with nominal diffraction angles of 144°, 120°, 90°, 60°, and 40° (left to right in this schematic) around the incident beam direction. The 144° panels of the same azimuth angle are typically combined together, resulting in 45 histograms. The tank in the center of the instrument has a volume of about 1 m^3 and can accommodate various sample environments. The large detector coverage allows to either probe 45 sample directions simultaneously for texture measurements [208, 209] or when data is appropriately merged to utilize the resulting short count times for kinetics studies.

for example, the development of models for the oxidation behavior in defective fuels [53]. Besides temperature, the oxygen partial pressure in the surrounding atmosphere also causes phase transformations, and the crystal structure of UO_{2+x} as a function of time and atmosphere during isothermal holding, for example, in situ oxidation or reduction, were studied by Desgranges et al. [54]. By clarifying the intermediate phases, such studies allow elucidating the phase transformation mechanisms.

3.2.2. Metallic Fuels. Neutrons have played a vital role in characterizing uranium and its alloys. As neutrons are also sensitive to ordering of magnetic moments, that is, the magnetic structure, neutrons are also used to probe whether magnetic ordering occurs in a given sample. Lander and Mueller [55] studied the crystal structure of orthorhombic α-uranium between 10 K and room temperature using single crystal neutron diffraction. The structure of tetragonal β-uranium, stable between 935 and 1045 K, was determined by Lawson et al. [56] using high-temperature neutron powder diffraction. Brown et al. utilized the engineering diffractometer SMARTS [57] to investigate the uniaxial deformation behavior of uranium at room temperature as well as 200°C and 400°C [58]. The large anisotropy of the orthorhombic α-uranium for deformation and thermal expansion, with a- and c-axes expanding with $\sim 20 \cdot 10^{-6}\,K^{-1}$ but a zero or even slightly negative expansion coefficient for the b-axis, makes such experiments valuable for characterization and understanding of the anisotropy.

Neutron diffraction was used by Birtcher et al. [59] to study the effects of neutron irradiation dose on the atomic structure of U_3Si_2, an intermetallic compound with application potential for high-power-density nuclear applications as well as reduced enrichment applications. In this material, neutron irradiation causes fission of the uranium atoms with the energetic fission products causing amorphous zones. It was found that for irradiation at room temperature these zones cause compressive lattice strains in the residual crystalline matrix with a linear dependence between strain and volume fraction of the amorphous phase. Ultimately total amorphization will occur. Neutron diffraction is the probe of choice here as the volume of the order of a cubic centimeter needs to be probed.

Spent fuel was characterized by Sears et al. [60] at the Chalk River neutron reactor source. Using a special container to shield the highly radioactive material, neutron diffraction data of the Al-U_3Si dispersion fuel was collected. Specimens from different regions of an actual fuel rod of the same reactor were measured to investigate the influence of power, temperature, and burn-up on the crystal structure and phase composition. The only diffraction signal of a crystalline phase observed was from the Al matrix, indicating that the U_3Si fuel particles and USiAl intermetallic reaction products formed during irradiation have become amorphous.

The U-10 wt% Mo metallic fuel used for instance as low enrichment replacement fuel for research reactors (Global Threat Reduction Initiative reactor convert program) was characterized by Seong et al. [61] as well as U-5.4 wt% Mo [62]. For this system, molybdenum is added to stabilize the cubic and therefore isotropic γ-uranium phase. However, at temperatures below ~580°C, both decomposition to α-uranium plus Mo-enriched γ-UMo and formation of metastable ordered U-Mo intermetallic phases lower the energy of the system. Formation of orthorhombic, highly anisotropic α-uranium is detrimental for the structural stability of the fuel foil. Therefore, studying the kinetics of the reactions during annealing at these temperatures is of great importance of the fabrication and application of such fuels. Neutrons, with their ability to study such materials in situ at temperature and with the large d-spacing range available to identify the metastable phases, have great value for

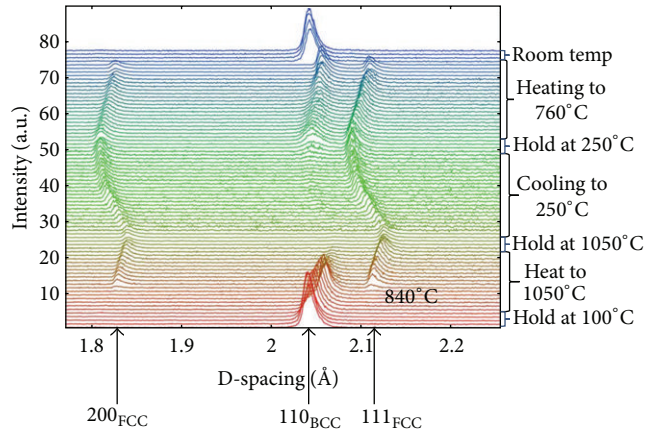

Figure 5: Changes in the neutron diffraction signal as a function of time and temperature for a HT-9 steel (after [63]). Some diffraction peaks of the ferrite (bcc) and austenite (fcc) phases are indicated. The disappearance of the ferrite and concurrent appearance of austenite peaks with increasing temperature as well as the change in peak positions due to temperature changes are visible. Data analysis allows to quantify these effects, for example, determination of volume fractions and lattice parameters/coefficients of thermal expansion of the two phases.

such studies. The time-temperature-transformation (TTT) diagrams used to characterize such processes are frequently generated by dilatometry or characterization after quenching followed by surface processing for metallography, XRD, or TEM. Dilatometry is not suitable for this particular system as both the decomposition and the repartitioning of Mo atoms cause length changes which cannot be deconvoluted to determine the fraction of residual γ phase.

3.3. Cladding. Zirconium and its alloys are extensively used in nuclear applications due to their good compromise of mechanical properties under high pressure/high temperature condition and neutron transparency. Its behavior during manufacturing and in service as well as under accident scenarios is therefore of great importance and a topic of extensive research. Pure zirconium has a hexagonal closed packed (hcp) crystal structure up to 866°C and transforms to a body-centered cubic (bcc) crystal structure at temperatures above. The main alloying elements for nuclear applications are niobium and tin, with the latter forming together with other minor elements, the so-called zircaloys (zircaloy is a trademark of Westinghouse Electric Company, Pittsburgh, PA, USA). Neutron diffraction has been applied to zirconium and its alloys to characterize welds, characterize deformation modes to allow predictive modeling of deformation, investigate the development of texture under temperature and stress, and characterize the phase transformations including texture variant selection during the hcp/bcc phase transformation. Besides zirconium and its alloys, steels are also investigated for cladding materials. The following sections describe some of these experiments.

3.3.1. Microstructural Characterization. Ferritic/martensitic steels such as T91 (9Cr1Mo) and HT-9 (12Cr1Mo) are candidate materials for nuclear reactor fuel cladding. Hosemann et al. [63] studied these materials using neutron diffraction. The evolution of the microstructure, that is, phase composition, texture, and so forth, was studied in situ using neutron diffraction. Such in situ measurements uniquely provide phase transition temperatures and kinetics and thermal expansion of the individual phases (Figure 5). From the determined coefficients of thermal expansion for each phase the thermal expansion of the bulk can be predicted using the observed phase fractions and compared to, for example, dilatometry measurements. Since thermal expansion, phase transformation, and redistribution of alloying elements all affect the volume, diffraction with its sensitivity to crystallographic phases provides a much more complete picture of the changes in the material than, for example, dilatometry. Neutron diffraction was also used by Hosemann et al. to characterize microstructural changes introduced by ion irradiation on these materials [64].

3.3.2. Deformation Studies. Due to the large interest in understanding the behavior of zirconium alloys for the nuclear industry, these materials became the subject of neutron diffraction applications very soon after neutron scattering became available for engineering-type studies. These studies go hand in hand with the development of polycrystalline deformation models, namely, both elastoplastic and viscoplastic self-consistent models [65], to understand and predict the deformation and grain-grain interactions during deformation in these highly anisotropic materials. In one of the earliest studies on this subject, MacEwen et al. [66] measured lattice-plane-dependent strains after 3.2% plastic deformation in tension and 1.2% in compression of zircaloy-2, elucidating the asymmetry of the response between tensile and compressive deformation. A benefit of neutron time-of-flight instruments for such measurements is the simultaneous availability of all measured lattice planes for a given sample direction (e.g., along the deformation axis), whereas in constant wavelength techniques the sample would have to be reoriented between measurements to accomplish the same with complications due to changes in interrogated volume, and so forth. Pang et al. [67] characterized the thermal residual stress state after thermomechanical treatment as well

as the stress tensor and intergranular stresses in situ during tensile deformation to 5% strain. For the interpretation of the lattice strains measured in such in situ deformation studies, elastoplastic self-consistent models are typically utilized and allow assessment of the activity of deformation modes such as slip and twinning.

For instance, Cai et al. [68] determined by neutron strain measurements the evolution of lattice strains during room-temperature deformation in tension and compression of a rolled and therefore textured Zr-2.5Nb plate. This material consists of hexagonal closed-packed α-phase and ~5% body-centered cubic β-phase. Neutron diffraction allows determination of strains and textures of both phases simultaneously and provides therefore a relatively complete picture of the material response to deformation. Several samples, cut with their deformation axis under different directions relative to the texture, were deformed into the plastic regime. Elastoplastic self-consistent modeling was applied to interpret the experimental data of the elastic and plastic deformation [69]. Determination of the single crystal elastic constants of the minority β-phase, for which single crystals are unavailable, from the experimental data-set illustrates the power of this method [70]. Cyclic loading in an engineering beamline allows to assess the microstructural evolution during repetitive application of the load [71] to study, for example, fatigue effects. Using the same approach, the effect of changes in the Nb concentration on the mechanical response can be also investigated [72].

The combination of viscoplastic self-consistent models and neutron texture measurements allows similar assessments also taking into account grain-reorientation during deformation; see, for example, Rangaswamy et al. [73]. Due to the anisotropy of the single crystals, in particular those of the hexagonal α phase, the orientation distribution or texture of the single crystals forming the polycrystalline aggregate is of great importance for the deformation behavior of zirconium alloys. Characterizing and ultimately predicting the texture evolution during thermomechanical processing steps and during service life are therefore active research areas. While cubic materials deform predominantly by slip, for noncubic materials twinning also plays an important role during deformation. Temperature [74, 75] as well as strain rate [76] influences the propensity of the deformation modes, and in situ diffraction studies are a unique tool to investigate the deformation behavior of such materials.

As an example, Figure 6 shows the texture evolution in Zr-2.5Nb measured on the HIPPO diffractometer [77, 78] using a high-temperature deformation furnace [79]. The texture of the 6 mm diameter and 20 mm long sample was measured at room temperature before and after the high-temperature deformation on a robotic sample changer [80] as a benchmark. During the furnace experiment, the texture was measured at 250°C, 625°C, 815°C, and 975°C, and then the sample was compressed by 20%, followed again by texture measurements at the same temperatures during cooling. In this material, the bcc β phase is metastable at room temperature. The volume fraction of the β phase increases during heating. The appearance of maxima in the 110 β pole figure at locations on the rim of the pole figure where the 0001 α pole figure shows maxima provides direct evidence for transformation of α grains to β grains rather than growth of preexisting β grains consuming α grains as is observed in other materials [81]. The deformation is performed at a temperature where only the bcc β phase exists, followed by cooling during which bcc grains transform to hcp α grains. Grains transforming from α phase to β phase follow the Burgers orientation relationship, which means that 0002 planes of the α phase become 110 planes of the β phase which is reflected in the texture evolution. During the phase transformation in polycrystalline aggregates, the so-called variant selection takes place which makes certain crystallographically equivalent variants fulfilling the Burgers orientation relationship more likely due to, for example, mechanical grain-grain interactions. The α/β phase transformation itself and the phenomenon of variant selection were also investigated using neutron diffraction for zirconium [82] and Zr-2.5Nb [83, 84]. In order to predict the phase transformation texture, the variant selection has to be understood, which is a field of active research. During the deformation in the pure β field, a typical bcc compression texture, orienting the 111 lattice planes preferentially with their normal along the compression direction, is observed. During cooling, again phase transformation textures following the Burgers orientation relationship and variant selection are observed. It is of paramount importance to be able to measure texture at intermediate steps during this simulation of thermomechanical treatment during processing of Zr-2.5Nb components. If only the pre- and postexperiment room temperature textures would be available, it would be impossible to deconvolute the influence of heating (leading to, e.g., recrystallization, not discussed here), phase transformations, variant selection, and deformation. Neutron diffraction has proven to be an unique and extremely valuable tool for such studies.

The presence of hydrides in zirconium-based alloys affects also their mechanical properties. Garlea et al. [85] studied the influence of hydrides on fatigue crack growth and compared hydride-free as-received Zircaloy-4 with the same material containing homogeneously distributed hydrides as well as inhomogeneously distributed hydrides resulting from a crack existing prior to the hydrogen charging. Among other characterization techniques, for all three cases, the residual stress field around the fatigue crack was characterized using neutron diffraction. From these measurements, it was found that the stress field of the preexisting crack influenced the formation of hydrides and therefore the mechanical behavior of the material.

3.4. Structural Materials. Materials used for pressure vessels or tubing outside the reactor core, such as steels, require understanding and ideally predictability of microstructural evolution, stress/strain evolution, and so forth, which can be obtained with neutron diffraction. In particular the thicknesses used for, for example, pressure vessels in the nuclear industry prevent other methods from successful application.

3.4.1. Residual Stress Measurements. As described by Withers et al. [86], until recently residual stresses have been included

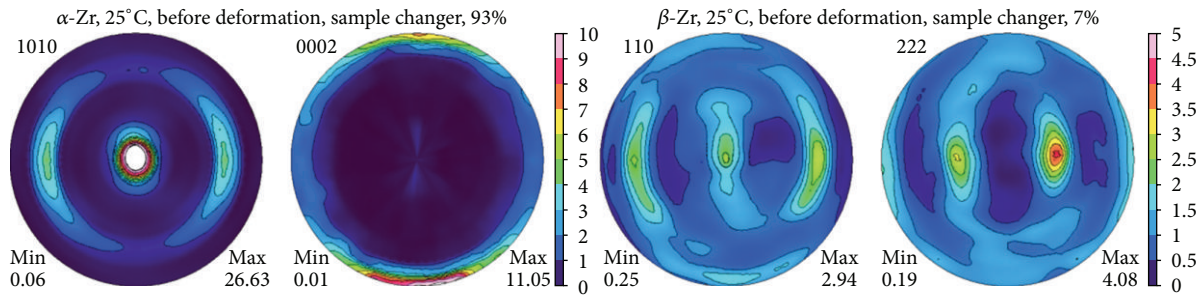

(a)

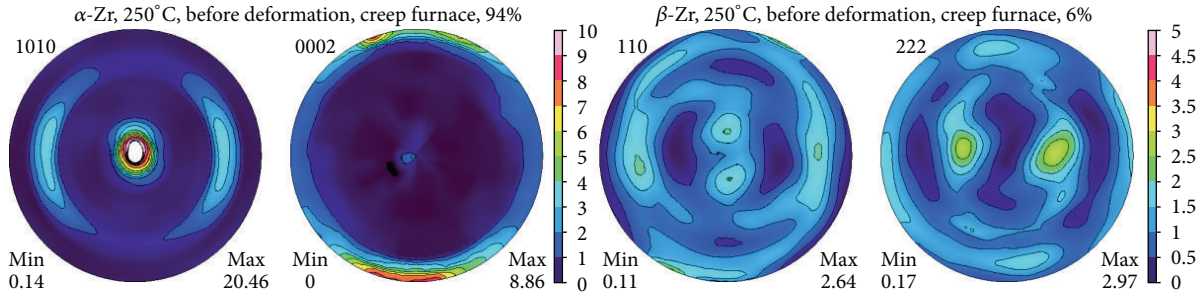

(b)

No α-phase at 975°C

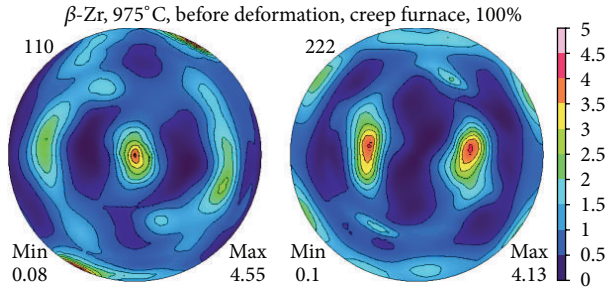

(c)

No α-phase at 975°C

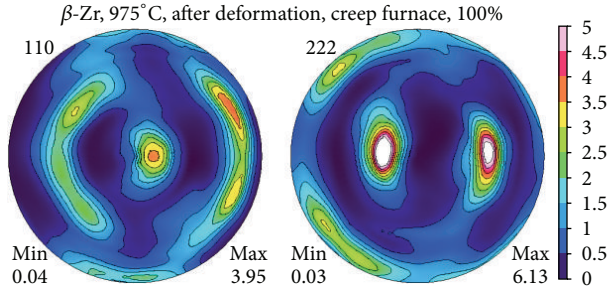

(d)

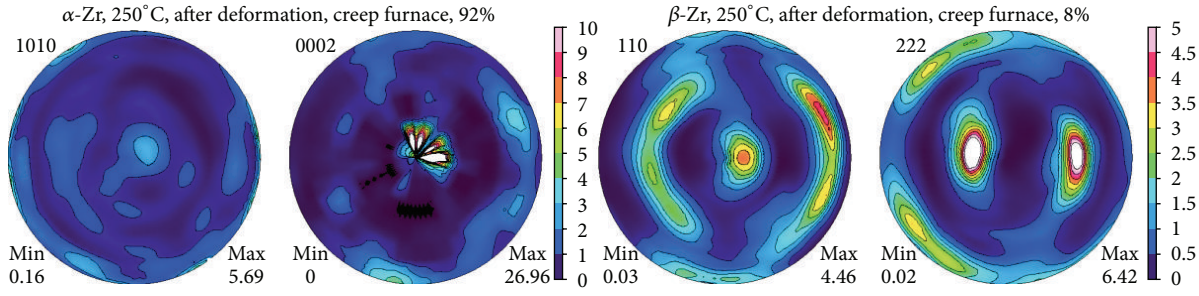

(e)

Figure 6: Continued.

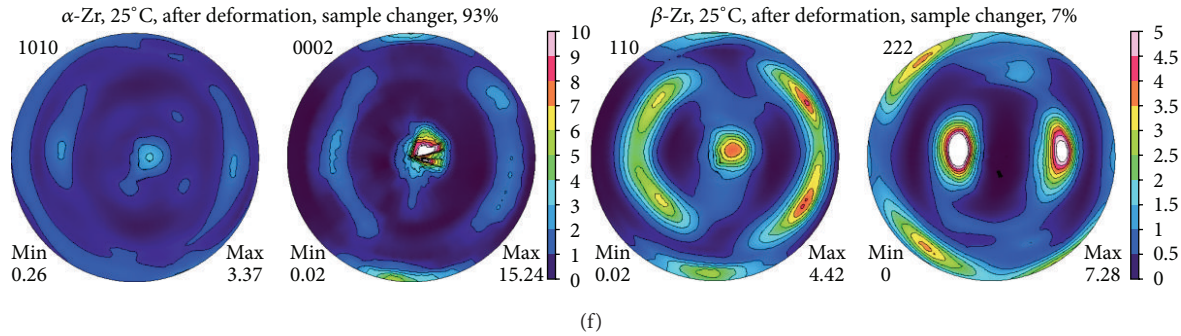

Figure 6: Texture evolution of α-phase (left column) and β-phase (right column) of Zr-2.5Nb at room temperature (a), 250°C (b), 975°C (c), after compression to 20% strain (d), cooling to 250°C (e), and again at room temperature (f) [79]. Allowing to measure the texture in situ at various temperatures and before and after the deformation in the β field uniquely allows to deconvolute the influences of temperature changes and deformation on the texture. Without this capability, only the two room temperature textures would be available.

in structural integrity assessments of nuclear pressure vessels and piping in a very primitive manner due to the lack of reliable residual stress measurement or prediction tools. The ability to quantify stresses from strain measurements by diffraction techniques and in particular by penetrating neutron diffraction is changing this situation. Due the higher fluxes available at modern neutron sources, three-dimensional mapping of the residual stresses or strains in actual or mock-up components becomes feasible. The experimental results may be used as input for structural integrity calculations or to validate finite element models on which safety cases for pressurized nuclear systems are founded.

Edwards et al. performed neutron diffraction strain measurements to quantify the three-dimensional residual stress field in a 20 mm thick stainless steel pipe girth weld containing a part-circumference "boat-shaped" weld repair [87]. Due to the ability to measure strains and therefore calculate stresses, it was possible to assess the residual stresses induced by the repair welding and it was found that, adjacent to the repair weld, the through-wall axial stress profile is membrane in character and of tensile magnitude equal to about 60% of the base metal 1% proof stress. From such experiments, repair procedures can be evaluated and in this particular case the measurements show that the repair procedure substantially increased axial and hydrostatic components of residual stress in the neighboring heat-affected zone. Systematically comparing pre- and postrepair stress fields allows to assess the effects of the repair procedures in more detail [88, 89].

Welding is also required to join parts of zirconium or its alloys together. During welding the maximum temperature is in the weld metal and decreases with increasing distance from the weld. Because of this temperature gradient, all processes that are influenced by temperature also possess gradients perpendicular to the weld. Due to the elastic and thermal anisotropy of the material, this introduces residual stresses of great importance to the application. Heat treatments are attempted to relieve the residual stresses, but their efficiency needs to be experimentally verified. The penetration of neutrons into zirconium allows measurement of lattice strains to evaluate the residual stresses as a function of location as is needed to determine stress profiles across a weld. In an exhaustive study, Carr et al. determined the residual stresses [90, 91] and the strain evolution during loading of the weld in a Zircaloy-4 weld using time-of-flight neutron diffraction from the measured lattice strains and the texture of the material [92]. Figure 7 shows some results of these studies.

3.4.2. Microstructural Characterization. For reactor applications, understanding and predictability of the evolution of the microstructure of structural materials at temperature and during irradiation are of great importance. Using neutron diffraction data from Zr-2.5% Nb specimen removed from a pressure tube which had been in service for seven years in a CANDU reactor at a temperature of ~250°C, Balogh et al. utilized profile analysis techniques [93] to determine the changes in dislocation types and densities with irradiation. Concurrent deformation studies of the irradiated and nonirradiated materials showed distinct differences in dislocation types introduced by plastic deformation between the irradiated and nonirradiated materials [94].

3.4.3. Deformation Studies. Deformation behavior of existing and proposed structural materials for nuclear reactors requires appropriate models and modeling parameters. Similar to the deformation studies on cladding materials, the deformation behavior of structural materials is investigated using neutron diffraction. Daymond and Bouchard utilized the ability of neutron diffraction to also probe the deformation behavior at elevated temperatures and investigated the response of 316 stainless steel to tensile loading at temperatures between 20°C and 650°C [95]. Again using elastoplastic self-consistent models, assessments of, for example, active slip systems, or the activity of different deformation modes as a function of temperature is possible in order to understand and ultimately predict the deformation or, for example, creep of components made from these materials.

The deformation behavior of the aforementioned HT-9 steels was investigated by Clausen et al. [96] using in situ

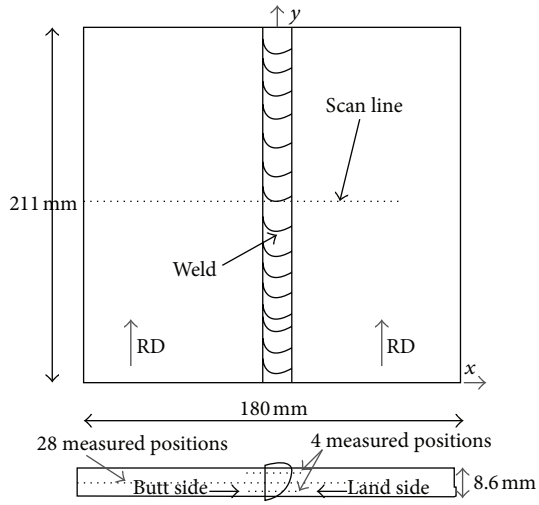

(a)

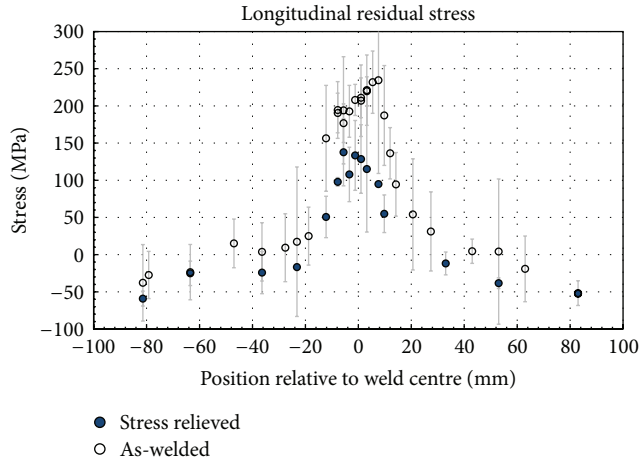

(b)

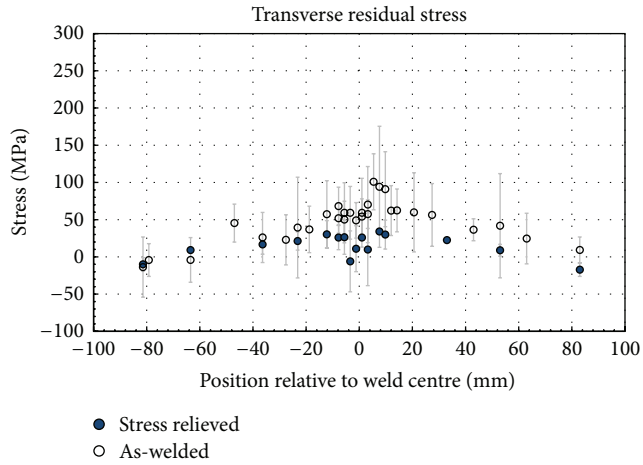

(c)

Figure 7: Continued.

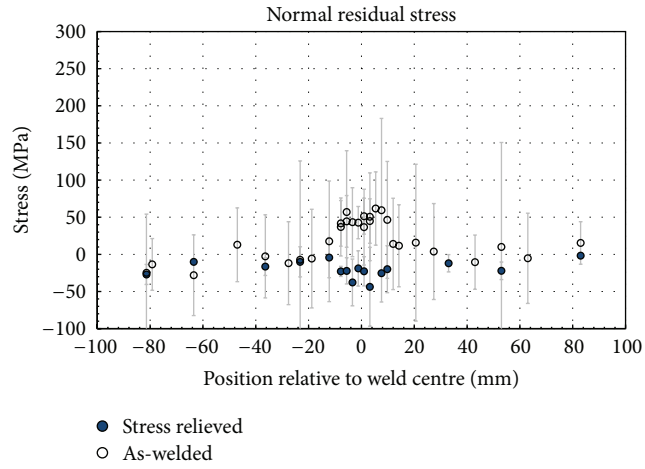

(d)

Figure 7: (a) Schematic of the linear butt-weld characterized by Carr et al. (adapted with permission from reference [90]). Variation of the macroscopic residual stresses along the three principal directions in a zircaloy-4 weld after a stress-relieving heat treatment (filled circles) and as-welded (open circles). The as-welded stresses are reduced by about 40% by the heat treatment. Measurements were taken across the plate (top) at the mid-thickness position (4.3 mm from either surface).

neutron diffraction and modeled using elastoplastic self-consistent (EPSC) modeling. These experiments on non-irradiated specimen provide baseline data for future similar experiments on irradiated materials. Comparing the mechanical response of irradiated and nonirradiated materials will allow to understand the influence of radiation damage on the mechanical behavior of these materials and provide benchmark data for advanced deformation models that attempt to include radiation damage [97].

3.5. Nuclear Waste Forms. Research of stable nuclear waste forms showed for instance that complex oxides are a possible form to lock radioactive atoms in stable lattices [98]. Research of these types of crystal structures naturally poses the same problems to crystal-chemistry studies as for nuclear fuels: the presence of both high (e.g., actinides) and low Z-number elements (oxygen in this case) biases the information gathered by electron, X-ray or synchrotron diffraction for, for example, determination of atomic positions heavily towards the high Z-number elements, while the structural response to, for example, cation substitution occurs also in the oxygen sublattice, such as distortion of the coordination polyhedra. Therefore, neutrons have been and will be an important probe to determine the crystal structures of candidate materials for nuclear waste forms and determine, for example, bond lengths, cation order/disorder, as well as comparing experimental structures with predicted ones, and so forth. However, typical irradiations by ions result in sample sizes much too small for neutron diffraction experiments; therefore only fundamental aspects of nonirradiated samples can be studied. In particular on pyrochlore structures considerable research was performed utilizing neutron diffraction [99–101].

3.6. Actinide-Bearing Minerals. For mining applications as well as prediction of crystal structures forming during accidents at nuclear power plants [39], knowledge and understanding of, for example, the thermal stability of the crystal structures of actinide-bearing minerals is of importance. Again, the presence of high and low Z-number elements makes neutron diffraction an important probe. Minerals such as Autunite ($Ca(UO_2)_2(PO_4)_2 \cdot 10$–$12H_2O$) or Torbernite ($Cu(UO_2)_2(PO_4)_2 \cdot 12\ H_2O$) also contain hydrogen, and studies of their decomposition to meta-autunite ($Ca(UO_2)_2(PO_4)_2 \cdot 6$–$8H_2O$) and metatorbernite ($Cu(UO_2)_2(PO_4)_2 \cdot 8\ H_2O$), respectively, add benefit to neutron diffraction studies as also the role of hydrogen atoms, governing the kinetics of the decomposition, can be studied in situ.

3.7. Outlook. The benefits of neutron diffraction for crystallographic studies of fuels, consisting of high and low Z-number elements, are obvious. Development of new fuels or advanced sample environments to study these materials at extreme conditions will continue. Few high temperature and controlled atmosphere experiments are reported thus far as well as only few high-temperature studies at temperatures above ~1500°C. Advances in sample environments as well as neutron sources will make such experiments more routine for the user at neutron facilities. As shown for the case of UC_2, such experiments provide unique data to verify theoretical predictions. Advanced diffraction data analysis techniques, such as the maximum entropy method developed for neutron diffraction data by Izumi and Momma [102, 103], will allow to study and revisit dynamic disorder of, for example, oxygen or carbon atoms in urania and uraniumcarbide, respectively. This method has been applied to experimentally visualize, for example, the diffusion path of Li ions in battery materials [104, 105]. Albeit it is experimentally certainly challenging, there is no reason to not apply this in the future to, for example, visualizing the diffusion of oxygen atoms to study

the Bredig transition in urania. Combinations of diffraction with the recently developed spatially resolved neutron time-of-flight detectors for energy-dispersive neutron radiography (see below) will open up entirely new avenues of neutron scattering research, which can be applied to nuclear materials.

4. Neutron Radiography

4.1. Introduction. Neutron radiography and tomography are based on the attenuation of neutron beams by the sample. As the interaction of neutrons with matter is fundamentally different from the interaction of X-rays with matter, neutrons allow investigations not feasible with other techniques such as visualization of hydrogen atoms even in operating systems. For instance, Takenaka et al. [106] and later Zboray et al. [107] investigated the annular flow of coolant liquid as well as the functional performance of a spacer system in a model system for a boiling water nuclear reactor fuel rod bundle using neutron tomography. Such imaging techniques are excellent tools to verify, understand, and optimize liquid flow in new designs.

Recent detector developments allowing for spatially and time-resolved neutron detection [108] are opening new avenues of characterization of nuclear materials and nuclear fuels in particular, as they allow for isotope-sensitive imaging via neutron resonance absorption imaging [109–115]. A program exploring advanced nondestructive examination (NDE) capabilities using neutron and proton imaging was initiated in 2011 between Los Alamos National Laboratory and Idaho National Laboratory. To illustrate the advantages of neutron radiography and energy-dispersive neutron radiography in particular, Figure 8 compares mock-up nuclear fuel rodlets, each consisting of five pellets prepared from urania powder and characterized by high-energy proton radiography, X-ray radiography [116], energy-dispersive neutron radiography, and thermal neutron radiography [117]. To simulate cracks and voids resulting from irradiation and burn-up in a fuel pin, plastic wire was embedded in the mock-up pellets which burned off during sintering leaving similar structures to voids and cracks. To assess the viability of detecting different isotopes, for example, fission products, tungsten pieces of different sizes and shapes were embedded in several fuel pins. Furthermore, some fuel pins were sintered with different green (presintering) densities. While both proton [118] and X-ray radiography are probing essentially gravimetric density variations, energy-dispersive neutron radiography allows to visualize, for example, the tungsten only by viewing the image at an energy where tungsten shows an absorption resonance. With proper calibrations, concentration measurements are possible.

The ultimate goal of the aforementioned collaboration is the characterization of irradiated fuel pins or even spent fuel. Both neutron and proton radiography have the benefit that either the detectors are inherently insensitive to the large amount of gamma radiation emitted or shielding can be installed between object and detector. For X-ray radiography, on the other hand, detectors have to be inherently sensitive to gamma radiation and discrimination between the probe used to characterize the material and the gamma radiation originating from radioactivity is much more difficult if not impossible. One goal of this collaborative effort is a better guidance for expensive destructive examination of irradiated fuel pins by the nondestructive characterization techniques. Similarly, besides stand-alone radiography and tomography, the combination of such characterization with neutron or synchrotron diffraction will open yet another avenue of future research [119] as regions of interest in bulk materials can be identified by radiography or tomography, followed by more detailed characterization with, for example, a general purpose neutron diffractometer (e.g., HIPPO [77, 78], GEM [120], POWGEN [121], iMATERIA [122], etc.), an engineering neutron diffractometer (e.g., SMARTS [58], ENGIN-X [123], Vulcan [124], TAKUMI [125], and Kowari [126]), or synchrotron X-ray micro-diffraction [127–129].

Besides concentration measurements, the neutron absorption resonances also allow remote sensorless temperature measurements [130–138], including the possibility to obtain three-dimensional temperature distributions from tomographic reconstruction [139, 140]. As high temperatures, potentially in combination with noninert (oxidizing or reducing) atmospheres, are desirable experimental conditions to investigate nuclear fuels under synthesis/processing or accident conditions, the sensorless temperature measurement via Doppler broadening of nuclear resonances provides an elegant mechanism to measure the sample temperature.

To illustrate these advantages, we first introduce the detectors used for this technique. Enabling technology for this new capability is a new class of high-resolution neutron counting detectors, enabling neutron resonance spectroscopy with 512 by 512 pixels (55 by 55 μm^2 each) and thus providing new possibilities of quantitative mapping of isotopic distributions within the samples [141] as well as remote spatially resolved temperature measurements [142]. The high spatial resolution resonance spectroscopy can only be realized with the presence of both a short-pulse intense neutron beam of the appropriate energy range, which is available at pulsed neutron spallation sources but not at typical reactor sources, and a neutron counting detector providing both spatial and temporal information for each detected neutron. Obviously, an energy scanning-type detector, such as a gated CCD imager, can also be used in principle, but such devices will require excessively long acquisition times as a large fraction of neutrons is gated out of each neutron pulse and only a small fraction of the neutron flux is registered by such a device. To properly fit the parameters of a neutron absorption resonance, a time resolution of an order of magnitude shorter than the neutron pulse width at the detector position, which is of the order of ~100–1000 ns, is required to resolve the narrow neutron resonance lines, especially at the energies exceeding 10 eV. While such excellent timing resolution has been demonstrated with a segmented detector using 2 by 2 mm^2 scintillators [143], such approach lacks the spatial resolution and limits the studies to a relatively coarse 2 mm accuracy. The novel detectors with neutron sensitive Microchannel Plates (MCPs) and Timepix [144] readout enable simultaneous detection of a large number of neutrons with spatial resolution of 55 μm^2 and temporal resolution

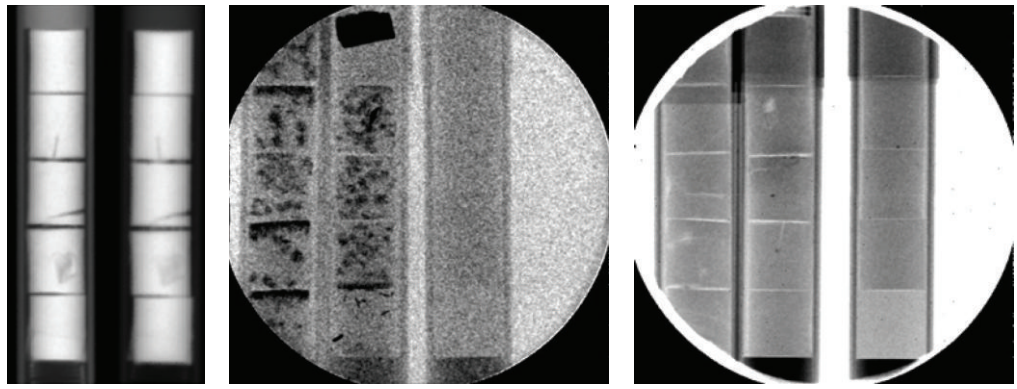

(a) (b) (c)

Figure 8: (a)–(c) Comparison of high-energy proton radiography, X-ray radiography (a) [116], energy-dispersive neutron radiography (b), and thermal neutron radiography (c) [117] of mock-up UO_2 fuel pins in stainless steel cladding with artificially introduced cracks or tungsten inclusions (visible as black areas in (b) by energy-dispersive neutron radiography).

as good as ~30 ns for epithermal neutrons and ~500 ns for thermal (limited by the depth of neutron absorption within 1 mm thick neutron absorbing MCP) [141]. The conversion of neutrons to electric signals occurs by means of absorption by specific isotopes dispersed into the MCP glass, such as ^{10}B. By choosing isotopes specific to the application, substantial enhancements in effective neutron absorption cross section and therefore detector efficiency can be achieved [145, 146]. It is worth pointing out that only spallation neutron sources operating in pulsed mode, which are at present ISIS (UK), J-PARC (Japan), SNS (USA), and LANSCE (USA), allow implementation of the neutron resonance absorption imaging technique. Source parameters to take into account are the initial neutron pulse width (affecting the energy resolution), shielding requirements (affecting the minimum source-detector distance and therefore the flux), and the repetition rate (affecting the maximum flight path length and therefore again the energy resolution). Because these neutron sources provide epithermal as well as thermal neutrons, high-resolution neutron resonance spectroscopy can be performed simultaneously to energy-resolved thermal-neutron imaging, thereby providing the possibility to measure crystallographic information for the sample at the same time as the isotopic distribution and temperature. The location of Bragg edges [147–152] in transmitted spectra can be used to map the integral of in-plane strain values [153–155], or, for example to reconstruct the phase map for samples with multiple phases. Quantitative phase analysis can elucidate which phases are present and what their volume fractions are [151, 156, 157]. Although there are limits to what transmission Bragg edge spectroscopy can provide, the combination of neutron resonance and transmission Bragg edge imaging enables some new and unique nondestructive characterization methods for nuclear materials. As the development of energy-dispersive neutron radiography just started, the remainder of this section reviewing neutron radiography applications to nuclear materials deals mostly with conventional thermal neutron radiography.

4.2. Fuel. The experimental procedures (including shielding considerations), detection methods, and resulting information when conventional (not energy-dispersive) thermal neutron radiography is applied to characterize nuclear fuel rods are described by Lehmann et al. [158]. Neutron and X-ray radiography for this particular purpose are also compared. The previous work by Groeschel et al. describes the handling concept and transfer cask in more detail [159]. Using conventional thermal neutron radiography, Lehmann et al. [160] and Vontobel et al. [161] characterized target rods from the Swiss spallation neutron source and could determine, for instance, the absence of substantial damage as well as hydrogen distributions, including hydrogen blisters, in the zircaloy and steel target rods. In particular, for fuels, energy-dispersive neutron radiography offers unparalleled characterization potential as, for instance, isotope concentrations, for example, from fission products, can be mapped out in three dimensions using tomographic reconstruction of the individual radiographs [117].

4.3. Cladding. Studying zirconium hydrides is of particular interest for accident scenarios, when the cladding material may react with cooling water. The interaction of H_2O with zirconium alloys is complex, as, for instance, oxygen stabilizes α-Zr, whereas hydrogen stabilizes β-Zr, therefore shifting phase transformation temperatures, while at the same time the solubility for hydrogen differs by an order of magnitude between α-Zr (6 at%) and β-Zr (50 at%) [162], leading to a complex temperature dependence of hydrogen uptake and release. Furthermore, large hydrogen concentrations may lead to blistering and once the dissolved hydrogen concentration at a given temperature exceeds the solubility, hydrides form, which are a major contributor to embrittlement. Obviously, inhomogeneities like cracks further complicate the problem.

The mechanisms of corrosion of zirconium-based alloys, in particular those relevant to in-reactor conditions, are despite decades of work still a field of active research. Neutron radiography has been utilized to measure the hydrogen concentration in various materials, including zirconium [163].

Yasuda et al. showed that sensitivities of 1000 wt ppm are possible for the detection of hydrogen in zirconium [164]. Sváb et al. [165] and Shaikh et al. [166] demonstrate the usefulness of combining neutron diffraction and radiography to identify the hydride phases and image their distribution in Zr-Nb alloys. Utilizing neutron radiography, Große et al. were able to quantify the kinetics [162] and spatial distribution [167] of hydrogen uptake in different zirconium-based alloys. For accident scenarios, high-temperature conditions are relevant, and the material behavior under such conditions was also studied by Große and coworkers [168, 169].

Other neutron-based techniques to measure the hydrogen concentration in metals and in particular in zirconium-based alloys to 10 wt ppm or better utilize the delayed neutron detection in a time-of-flight experiment due to decreased energy after inelastic scattering by hydrogen [170, 171], incoherent scattering [172], or cold neutron prompt gamma activation analysis [173]. However, while providing similar accuracy for the hydrogen concentration determination, these techniques are not suitable for imaging and rather provide the bulk average from the volume illuminated by the incident neutron beam.

Utilizing the novel detectors developed by Tremsin et al. described above, Santisteban et al. [174] imaged the texture changes in zirconium-based components. Such measurements allow to characterize gradients in preferred orientation in pressure tubes, rolled plates, or around welds. In combination with stress/strain and grain size measurements, such spatially resolved information on the bulk microstructure provides unique insights into microstructural changes during thermomechanical processing and valuable data to benchmark applicable simulations attempting to model such processing.

4.4. Outlook. Imaging is an integral part of the instrument suite at recently commissioned as well as future neutron sources [175]. In particular energy-dispersive neutron imaging, as the required detector technology became available only recently, is still in its infancy, and expected advances in experimental setups and data analysis have great promise in particular when applying energy-dispersive neutron radiography to nuclear materials. Detector efficiency can be greatly improved by doping the scintillator glass with the isotopes of interest. As of now, no dedicated beamline for this technique exists; therefore, reductions in background and substantial improvements in beam optics can be expected. Implementation of Kirckpatrick-Baez neutron mirrors [176, 177] for beam focusing to allow resolution improvements in regions of interest determined with the open beam should be possible. In particular for the data analysis one can expect great advances when adaption to energy-dispersive neutron tomography of methods recently developed for tomographic reconstruction of medical CT-scans, such as limited view angle iterative CT reconstruction [178], model-based image reconstruction [179], or Markov random fields [180], is explored. With improved sensitivity, accurate measurements of isotope concentrations will be possible, which will allow to study, for example, the motion of chloride or uranium atoms in concrete to understand ion migration in concrete, which is a complex interplay of chemical interactions and capillary flow in cavities. Testing of additions to the concrete to inhibit migration of, for example, chloride or uranium ions to prevent corrosion or contamination, respectively, will also be possible.

5. Other Neutron Techniques

In this section we cover some neutron scattering techniques less frequently utilized to characterize nuclear materials, such as small angle scattering, reflectometry, diffuse scattering, or total cross-section measurements.

5.1. Small Angle Neutron Scattering. Small angle neutron scattering (SANS) probes mesoscopic length scale structures between ~1 and 1000 nm by analyzing the scattering into small scattering angles. Utilizing the change in refractive index due to changes in scattering density, shapes, and sizes of precipitates, voids, and so forth, can be probed nondestructively.

Utilizing SANS at the PAXY instrument [181] at the Laboratoire Léon Brillouin, Saclay, France, Mathon et al. investigated redistribution of chromium in martensitic steels under irradiation at temperatures between 250 and 400°C [182]. They found a phase separation for chromium concentrations above a threshold value of ~7.2 at% at 325°C and studied the influence of irradiation dose and temperature as well as the influence of other alloying elements on this effect. As they point out, for studying precipitation at the nanometer scale in ferromagnetic martensitic/ferritic steels, small angle neutron scattering (SANS) is in some specific cases more powerful than transmission electron microscopy (TEM). This may be either because of a more favorable contrast between precipitates and matrix or when the particles are very small (<5 nm). Furthermore, SANS probes a sample volume many orders of magnitude larger than TEM and is not subject to problems from sample preparation.

A high density of nanoscale clusters of YTiO in ferritic alloys results in superior creep strength and the potential for high resistance to radiation damage. To study fabrication of such materials, Alinger and coworkers studied the development and stability of YTiO nanoclusters in mechanically alloyed FeCr-based ferritic alloys [183] using SANS. The thermal stability of the clusters in the ferritic alloy matrix was also investigated.

Bouchard et al. utilized SANS to map the level of creep cavitation around a surface breaking crack in a stainless steel pressure vessel which had been in service for 65,000 h at an operating temperature of around 525°C. Such experimental data allows to validate prediction of applicable models for creep cavitation failure [184].

Anderoglu et al. studied the microstructure and phase evolution in a fully tempered ferritic/martensitic HT-9 steel irradiated in the Fast Flux Test Reactor Facility (FFTF) up to 155 dpa at a temperature range of 380 to 504°C [185] using small angle neutron scattering at the LQD instrument [186] at LANSCE among other techniques. Microstructural

parameters such as grain or void sizes may be characterized as a function of dose and temperature.

5.2. Neutron Transmission Measurements. Modeling of reactors depends on the precise knowledge of interaction cross sections of thermal neutrons with reactor materials. These cross sections are energy-dependent and in particular in the thermal neutron energy range an overlay of coherent and incoherent inelastic and elastic scattering as well as continuous and resonant absorption. Especially intense pulsed spallation neutron sources allow rapid cross-section measurements in the thermal energy region for reactor materials. Even the cross sections for materials used for decades in nuclear applications such as graphite still require improvements as shown recently by Bowman et al. [187]. Obviously, complimentary characterization using neutron diffraction method to establish phases, texture, and so forth of the same materials provides valuable additional information for such measurements.

Utilizing the neutron absorption resonances described in Section 4, Lynn et al. [188] measured the vibrational properties of atoms in a δ-phase (face-centered cubic crystal structure) Pu-3.6 at.% Ga alloy by quantifying the Doppler-broadening of the neutron absorption resonances due to the motion of the atoms as a function of temperature between 15 and 303 K. Such measurements allow to measure, for example, the first and second moments of the phonon spectrum and the Debye temperature of each atom. This in turn allows to compare the vibrations of atoms in the alloy with the same atoms in pure phases to study differences in local environments, detecting, for instance, potential clustering of alloyed elements. Recent theoretical simulations of the phonon spectra were successful in predicting atomic displacement experimentally determined by neutron diffraction in moderately complex structures such as the MAX phases, which are nanolamellar ternary carbides [189]. Utilizing the experimental techniques developed by Lynn et al. would provide another approach to provide experimental data to compare phonon simulations that has not been explored yet. In combination with the spatially resolved detectors described also in Section 4, one could envision for the first time spatially resolved measurements of thermodynamic properties such as the first and second moments of the phonon spectra of atoms. This could be in turn applied to nuclear fuel materials, such as uraniumdioxide, under an applied temperature gradient.

5.3. Diffuse Scattering. Besides Bragg diffraction, where the crystallographic information is derived from the integrated peak intensities via the structure factor, diffuse scattering from UO_2 or ThO_2 single crystals can be used to study disorder and oxygen diffusion; see, for example, Clausen et al. [190, 191] and Goff et al. [192]. It is important to note that these measurements had to be performed in situ at temperatures up to 2930 K to study the diffusion, which required development of a special furnace at the ISIS facility [193]. From the same data, both diffuse scattering and diffraction can be obtained, which allowed simultaneous measurements of structural parameters such as lattice parameters and thermal parameters. See also the review article by Hutchings [194] for a review of earlier neutron scattering work on UO_2 and ThO_2 at Harwell and Risø. It is important to stress that the phases and their behavior have to be studied in situ as the phenomena relevant to operation and accident conditions are temperature activated.

Pair distribution function (PDF) analysis measures atomic distances and the probability to find an atom at a distance r from another atom [195]. PDF analysis does not rely on periodicity of the atomic arrangement and can thus, besides applying it to study liquids and glasses, be used to probe the local atomic structure, that is, small distortions from the average periodic crystal structure probed by powder diffraction. To study radiation damage in a glass, Wright et al. [196] compared the structure of vitreous silica before and after neutron irradiation to a dose of 2.8×10^{20} fast neutrons/cm^2 using pair-distribution functions. They found an increase in Si–O bond length, consistent with the observed macroscopic increase in density. The crystal structure of α-U_4O_9 was analyzed using pair distribution function analysis from neutron scattering data by Garrido et al. [197] to verify findings on the U–O bond lengths derived from EXAFS results by Conradson et al. [198]. Disagreement was found, illustrating how tackling a crystal structure problem with different methods may advance science. The low temperature phase α-U_4O_9 was investigated using neutron pair distribution functions by Desgranges et al. [199]. It was found that cubic β-U_4O_9 upon cooling undergoes a trigonal distortion to form α-U_4O_9. From these results new insight into the formation mechanism of U_3O_8 could be obtained, illustrating the power of detailed crystallographic analysis.

5.4. Inelastic Scattering. As the energy of thermal neutrons is similar to the generation or annihilation energies for phonons, neutrons can also be used to probe the lattice dynamics of nuclear materials. The first phonon dispersion curve for UO_2 at room temperature was measured by Dolling et al. [200] at the Chalk River reactor. Using inelastic neutron scattering at LANSCE, McQueeney et al. measured the phonon density of states and adiabatic sound velocities of fcc-stabilized $^{242}Pu_{0:95}Al_{0:05}$ [201]. With increasing temperature it was found that the phonon frequencies and sound velocities decrease considerably, despite negligible thermal expansion. The complex electronic structure as a function of temperature of Pu was considered as a possible explanation for this unusual phonon softening.

5.5. Neutron Reflectometry. Using the neutron reflectometer SPEAR at LANSCE [202], He et al. [203] characterized the surface of an ultrathin (<100 nm thickness) film of uranium oxide UO_x deposited on a quartz substrate. This technique allows to measure thicknesses and scattering characteristics of homogeneous layers. From the scattering characteristics, the chemistry can be determined. The thicknesses are measured with 0.1 nm resolution. He et al. found that the film was composed of three sublayers: A ~38 Å thick layer of U_3O_8 formed along the UO_x/SiO_2 substrate interface, a second

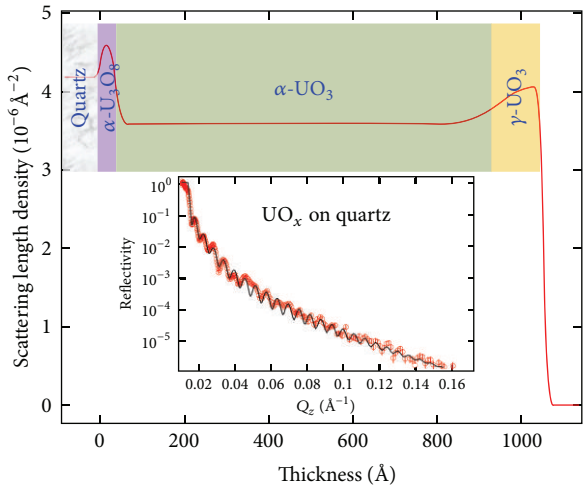

FIGURE 9: Layer thicknesses of different urania phases as derived from differences in scattering length densities obtained in a neutron reflectometry experiment. The inset shows the neutron reflectivity data as circles with the model fit (after [203]).

sublayer consisting of ~900 Å thick single phase of α-UO_3, and a top layer of γ-UO_3 with a thickness of ~115 Å (Figure 9). It can be envisioned that such measurements can be utilized to study oxidation and reduction characteristics on sub-nanometer lengths scales by characterizing similar samples exposed to different durations in a controlled atmosphere.

6. Summary and Outlook

Neutron scattering techniques have played and are still playing a vital role in characterizing materials of relevance to nuclear energy generation. In particular, for nuclear fuels, where high and low Z-number elements are combined, neutron diffraction has inherent advantages over, for example, X-ray diffraction due to the differences in interaction between beam and atoms in the sample. Support for potential users at various international user facilities, as listed in Section 2, is available, and researchers interested in such experiments should not hesitate to contact beam-line scientists at these facilities.

Energy-dispersive neutron radiography is in its infancy, and expected advances in experimental setup and data analysis have great promise in particular when applying this technique to nuclear materials. Three-dimensional tomographic reconstruction of quantities not accessible by any other nondestructive technique, such as isotope concentrations or temperatures, offers great promises for future applications of this technique. As the required nuclear resonances are naturally available in the materials of interest to the nuclear materials community, such materials are immediate candidates for applications of this evolving technique.

Main trends which can be expected to continue are advances in neutron flux and detector coverage, allowing faster acquisition times, for example, kinetics studies or smaller samples. Sample environments will continue to be developed to study in particular changes in nuclear materials under high temperature and controlled atmosphere conditions. Characterization of highly radioactive materials, such as specimen from irradiated components, will become possible once either shielding containers or dedicated beam-lines for such materials become available. Combinations of techniques, such as diffraction and radiography, will provide detailed crystallographic information in combination with spatially resolved distribution of the properties of interest. Combined characterization at large-scale facilities, for instance, characterization of density using proton radiography, isotope distribution by energy-dispersive neutron radiography, phase composition, and texture using neutron diffraction are in principle possible at facilities like LANSCE and utilize the unique penetration ability to characterize, for example, irradiated fuel pins inside a shielding container. Such combinations will increase the return of investment for transporting highly radioactive materials from the irradiation facility to the characterization facility. Studying materials under extreme conditions is also expected to grow: measuring the viscosity of molten urania or even Corium as a function of temperature using proton radiography, mimicking the falling sphere experiments developed by Winkler et al. for measuring viscosity of rock melts using neutron radiography [210–212], would provide unique data not available otherwise. Using pair-distribution function analysis, the atomic arrangement in the melts could be studied using neutron scattering. Integration of neutron scattering facilities with irradiation facilities, such as the proposed MaRIE (Matter-Radiation Interactions in Extremes) facility at LANL [213–215], will open up yet another new avenue of research.

Acknowledgments

The author thanks Professor Peter Hosemann (Department of Nuclear Engineering, University of California, Berkeley), Drs. Jarek Majewski, Matt Reiche, Peng Wang (LANSCE, LANL), and Dr. Winfried Kockelmann (ISIS, Rutherford Appleton Laboratory) for their contributions. The permission by Nuclear Power Today (http://www.world-nuclear.org/) to use Figure 1 and by David Carr (Institute of Materials and

Engineering Science, ANSTO) to use Figure 7 for this paper is appreciated. Special thanks go to a dear friend for inspiring and motivating this paper.

References

[1] Nuclear Power Today, 2012, http://www.world-nuclear.org/info/inf01.html.

[2] Nuclear Energy Institute, 2012, http://www.nei.org/resourcesandstats/nuclear_statistics/usnuclearpowerplants.

[3] Nuclear Power Today, 2013, http://www.world-nuclear.org/info/inf08.html.

[4] J. M. Carpenter and G. H. Lander, "40 years of neutron scattering: a perspective," *Neutron News*, vol. 21, pp. 10–12, 2010.

[5] W. G. Stirling and C. Vettier, "The most useful microscopic probes—neutrons and synchrotron X-rays," *Neutron News*, vol. 21, no. 1, pp. 13–17, 2010.

[6] W. Mampe, P. Ageron, C. Bates, J. M. Pendlebury, and A. Steyerl, "Neutron lifetime measured with stored ultracold neutrons," *Physical Review Letters*, vol. 63, no. 6, pp. 593–596, 1989.

[7] R. Pynn, "Neutron scattering: a primer," *Los Alamos Science*, vol. 19, pp. 1–31, 1990, http://library.lanl.gov/cgi-bin/getfile?00326651.pdf.

[8] L. Dobrzyński and K. Blinowski, *Neutrons and Solid State Physics*, Ellis Horwood Series: Physics (editor: M. Cooper), Ellis Horwood, 1994.

[9] A. J. Dianoux and G. Lander, *Neutron Data Booklet*, Institut Laue-Langevin, 2002.

[10] S. C. Vogel and H. G. Priesmeyer, "Neutron production, neutron facilities and neutron instrumentation," *Reviews in Mineralogy and Geochemistry*, vol. 63, pp. 27–57, 2006.

[11] S. C. Vogel and J. S. Carpenter, "Brief introduction to neutron scattering and global neutron user facilities," *JOM: Journal of the Minerals, Metals and Materials Society*, vol. 64, no. 1, pp. 104–111, 2012.

[12] "International Workshop on Scattering Techniques for Structural Materials at UC Berkeley," 2013, http://scatter.nuc.berkeley.edu/.

[13] Institut Laue-Langevin, 2013, http://www.ill.eu/.

[14] OPAL, "ANSTO's research reactor," 2013, http://www.ansto.gov.au/AboutANSTO/OPAL/index.htm.

[15] S. J. Kennedy, "Construction of the neutron beam facility at Australia's OPAL research reactor," *Physica B*, vol. 385-386, part 2, pp. 949–954, 2006.

[16] National Research Universal (NRU), 2013, http://www.nrucanada.ca/en/home/default.aspx.

[17] B. Powell, "Neutron scattering at Chalk River," *Neutron News*, vol. 1, pp. 16–20, 1990.

[18] FRM II, "Forschungs-Neutronenquelle Heinz Maier-Leibnitz (FRM II)," 2013, http://www.frm2.tum.de/en/index.html.

[19] "The High Flux Isotope Reactor at Oak Ridge National Laboratory," 2013, http://neutrons.ornl.gov/facilities/HFIR/.

[20] M. Yethiraj and J. A. Fernandez-Baca, "Neutron scattering at the high flux isotope reactor at Oak Ridge national laboratory," *Materials Research Society Symposium Proceedings*, vol. 376, pp. 59–70, 1995.

[21] NIST Center for Neutron Research, 2013, http://www.ncnr.nist.gov/.

[22] R. Cappelletti, "The national institute of standards and technology center for neutron research (NCNR)," *Neutron News*, vol. 12, pp. 10–14, 2001.

[23] Neutron Scattering Facilities, 2013, http://www.neutron.anl.gov/facilities.html.

[24] "About Laboratory : Frank Laboratory of Neutron Physics," 2013, http://flnp.jinr.ru/25/.

[25] A. V. Belushkin, "IBR-2-the fast pulsed reactor at Dubna," *Neutron News*, vol. 2, pp. 14–18, 1991.

[26] Paul Scherrer Institut (PSI), "Swiss Spallation Neutron Source—SINQ," 2013, http://www.psi.ch/sinq/.

[27] G. S. Bauer, "Operation and development of the new spallation neutron source SINQ at the Paul Scherrer Institut," *Nuclear Instruments and Methods in Physics Research B*, vol. 139, no. 1–4, pp. 65–71, 1998.

[28] Los Alamos Neutron Science Center, 2013, http://lansce.lanl.gov/.

[29] P. W. Lisowski and K. F. Schoenberg, "The Los Alamos neutron science center," *Nuclear Instruments and Methods in Physics Research A*, vol. 562, no. 2, pp. 910–914, 2006.

[30] ISIS Home Page, 2013, http://www.isis.stfc.ac.uk/.

[31] J. Agbenyega and M. Bull, "A world of neutrons & muons," *Materials Today*, vol. 12, no. 7-8, p. 59, 2009.

[32] Neutron Sciences at Oak Ridge National Laboratory, 2013, http://www.sns.gov/.

[33] T. E. Mason, D. Abernathy, J. Ankner et al., "The spallation neutron source: a powerful tool for materials research," in *AIP Conference Proceedings*, vol. 773, pp. 21–25, 2004.

[34] "J-PARC—Japan Proton Accelerator Research Complex," 2013, http://j-parc.jp/index-e.html.

[35] Y. Ikeda, "Current status of 1 MW pulse spallation neutron source (JSNS) of J-PARC," *Journal of Nuclear Materials*, vol. 343, no. 1–3, pp. 7–13, 2005.

[36] ESS (Home), 2013, http://europeanspallationsource.se/.

[37] China Spallation Neutron Source, 2013, http://csns.ihep.ac.cn/english/index.htm.

[38] W. Jie, F. Shi-Nian, T. Jing-Yu et al., "China spallation neutron source—an overview of application prospects," *Chinese Physics C*, vol. 33, no. 11, pp. 1033–1042, 2009.

[39] P. C. Burns, R. C. Ewing, and A. Navrotsky, "Nuclear fuel in a reactor accident," *Science*, vol. 335, no. 6073, pp. 1184–1188, 2012.

[40] A. Bowman, G. Arnold, W. Witteman, T. Wallace, and N. Nereson, "The crystal structure of UC_2," *Acta Crystallographica*, vol. 21, part 5, pp. 670–671, 1966.

[41] M. Bredig, "The crystal structure of UC_2," *Journal of the American Ceramic Society*, vol. 43, no. 9, pp. 493–494, 1960.

[42] W. Wilson, "The crystal structure of UC_2," *Journal of the American Ceramic Society*, vol. 43, no. 2, pp. 77–80, 1960.

[43] T. B. Massalski, H. Okamoto, P. Subramanian, and L. Kacprzak, *Binary Alloy Phase Diagrams*, vol. 3, ASM International, 1990.

[44] X. D. Wen, S. P. Rudin, E. R. Batista, D. L. Clark, G. E. Scuseria, and R. L. Martin, "Rotational rehybridization and the high temperature phase of UC_2," *Inorganic Chemistry*, vol. 51, no. 23, pp. 12650–12659, 2012.

[45] B. T. M. Willis, "Positions of the oxygen atoms in $UO_{2.13}$," *Nature*, vol. 197, no. 4869, pp. 755–756, 1963.

[46] A. F. Andresen, "The structure of U_3O_8 determined by neutron diffraction," *Acta Crystallographica*, vol. 11, part 9, pp. 612–614, 1958.

[47] B. Loopstra, "Neutron diffraction investigation of U_3O_8," *Acta Crystallographica*, vol. 17, part 6, pp. 651–654, 1964.

[48] D. J. M. Bevan, I. E. Grey, and B. T. M. Willis, "The crystal structure of β-U_4O_{9-y}," *Journal of Solid State Chemistry*, vol. 61, no. 1, pp. 1–7, 1986.

[49] R. I. Cooper and B. T. M. Willis, "Refinement of the structure of β-U_4O_9," *Acta Crystallographica A*, vol. 60, no. 4, pp. 322–325, 2004.

[50] B. O. Loopstra, J. C. Taylor, and A. B. Waugh, "Neutron powder profile studies of the gamma uranium trioxide phases," *Journal of Solid State Chemistry*, vol. 20, no. 1, pp. 9–19, 1977.

[51] A. Belsky, M. Hellenbrandt, V. L. Karen, and P. Luksch, "New developments in the inorganic crystal structure database (ICSD): accessibility in support of materials research and design," *Acta Crystallographica B*, vol. 58, no. 3, pp. 364–369, 2002.

[52] J. D. Higgs, W. T. Thompson, B. J. Lewis, and S. C. Vogel, "Kinetics of precipitation of U_4O_9 from hyperstoichiometric UO_{2+x}," *Journal of Nuclear Materials*, vol. 366, no. 3, pp. 297–305, 2007.

[53] J. D. Higgs, B. J. Lewis, W. T. Thompson, and Z. He, "A conceptual model for the fuel oxidation of defective fuel," *Journal of Nuclear Materials*, vol. 366, no. 1-2, pp. 99–128, 2007.

[54] L. Desgranges, G. Baldinozzi, G. Rousseau, J. C. Nièpce, and G. Calvarin, "Neutron diffraction study of the in situ oxidation of UO_2," *Inorganic Chemistry*, vol. 48, no. 16, pp. 7585–7592, 2009.

[55] G. Lander and M. Mueller, "Neutron diffraction study of α-uranium at low temperatures," *Acta Crystallographica B*, vol. 26, part 2, pp. 129–136, 1970.

[56] A. Lawson, C. Olsen, J. Richardson, M. Mueller, and G. Lander, "Structure of α-uranium," *Acta Crystallographica B*, vol. 44, pp. 89–96, 1988.

[57] D. W. Brown, M. A. M. Bourke, B. Clausen et al., "Temperature and direction dependence of internal strain and texture evolution during deformation of uranium," *Materials Science and Engineering A*, vol. 512, no. 1-2, pp. 67–75, 2009.

[58] M. A. M. Bourke, D. C. Dunand, and E. Ustundag, "SMARTS—a spectrometer for strain measurement in engineering materials," *Applied Physics A*, vol. 74, no. 1, supplement, pp. s1707–s1709, 2002.

[59] R. C. Birtcher, J. W. Richardson Jr., and M. H. Mueller, "Amorphization of U_3Si_2 by ion or neutron irradiation," *Journal of Nuclear Materials*, vol. 244, no. 3, pp. 251–257, 1997.

[60] D. Sears, N. Wang, R. Rogge, I. Swainson, and R. Donaberger, "Neutron Diffraction Analysis of High Burnup LEU Fuel from NRU," 2011, http://www.cins.ca/docs/exp_rep/CNBC-2011-MS-5.pdf.

[61] B. S. Seong, C. H. Lee, J. S. Lee et al., "Neutron diffraction study of U-10 wt% Mo alloy," *Journal of Nuclear Materials*, vol. 277, no. 2-3, pp. 274–279, 2000.

[62] J. S. Lee, C. H. Lee, K. H. Kim, and V. Em, "Neutron diffraction study of U-5.4 wt% Mo alloy," *Journal of Nuclear Materials*, vol. 280, no. 1, pp. 116–119, 2000.

[63] P. Hosemann, S. Kabra, E. Stergar, M. J. Cappillo, and S. A. Maloy, "Micro-structural characterization of laboratory heats of the Ferric/Martensitic steels HT-9 and T91," *Journal of Nuclear Materials*, vol. 403, no. 1–3, pp. 7–14, 2010.

[64] P. Hosemann, C. Vieh, R. R. Greco et al., "Nanoindentation on ion irradiated steels," *Journal of Nuclear Materials*, vol. 389, no. 2, pp. 239–247, 2009.

[65] U. F. Kocks, C. N. Tomé, and H. R. Wenk, *Texture and Anisotropy: Preferred Orientations in Polycrystals and Their Effect on Materials Properties*, Cambridge University Press, New York, NY, USA, 2000.

[66] S. R. MacEwen, J. Faber Jr., and A. P. L. Turner, "The use of time-of-flight neutron diffraction to study grain interaction stresses," *Acta Metallurgica*, vol. 31, no. 5, pp. 657–676, 1983.

[67] J. W. L. Pang, T. M. Holden, P. A. Turner, and T. E. Mason, "Intergranular stresses in Zircaloy-2 with rod texture," *Acta Materialia*, vol. 47, no. 2, pp. 373–383, 1999.

[68] S. Cai, M. R. Daymond, R. A. Holt, M. A. Gharghouri, and E. C. Oliver, "Evolution of interphase and intergranular stresses in Zr-2.5Nb during room temperature deformation," *Materials Science and Engineering A*, vol. 501, no. 1-2, pp. 166–181, 2009.

[69] S. Cai, M. R. Daymond, and R. A. Holt, "Modeling the room temperature deformation of a two-phase zirconium alloy," *Acta Materialia*, vol. 57, no. 2, pp. 407–419, 2009.

[70] S. Cai, M. R. Daymond, A. K. Khan, R. A. Holt, and E. C. Oliver, "Elastic and plastic properties of βZr at room temperature," *Journal of Nuclear Materials*, vol. 393, no. 1, pp. 67–76, 2009.

[71] S. Cai, M. R. Daymond, R. A. Holt, and E. C. Oliver, "Evolution of internal strains in a two phase zirconium alloy during cyclic loading," *Acta Materialia*, vol. 59, no. 13, pp. 5305–5319, 2011.

[72] S. Cai, M. R. Daymond, and R. A. Holt, "Deformation of high β-phase fraction Zr-Nb alloys at room temperature," *Acta Materialia*, vol. 60, no. 8, pp. 3355–3369, 2012.

[73] P. Rangaswamy, M. A. M. Bourke, D. W. Brown et al., "A study of twinning in zirconium using neutron diffraction and polycrystalline modeling," *Metallurgical and Materials Transactions A*, vol. 33, no. 3, pp. 757–763, 2002.

[74] C. N. Tomé, P. J. Maudlin, R. A. Lebensohn, and G. C. Kaschner, "Mechanical response of zirconium—I. Derivation of a polycrystal constitutive law and finite element analysis," *Acta Materialia*, vol. 49, no. 15, pp. 3085–3096, 2001.

[75] G. C. Kaschner, J. F. Bingert, C. Liu et al., "Mechanical response of zirconium—II. Experimental and finite element analysis of bent beams," *Acta Materialia*, vol. 49, no. 15, pp. 3097–3108, 2001.

[76] T. A. Sisneros, D. W. Brown, B. Clausen et al., "Influence of strain rate on mechanical properties and deformation texture of hot-pressed and rolled beryllium," *Materials Science and Engineering A*, vol. 527, no. 20, pp. 5181–5188, 2010.

[77] H. R. Wenk, L. Lutterotti, and S. Vogel, "Texture analysis with the new HIPPO TOF diffractometer," *Nuclear Instruments and Methods in Physics Research A*, vol. 515, no. 3, pp. 575–588, 2003.

[78] S. C. Vogel, C. Hartig, L. Lutterotti, R. B. Von Dreele, H. R. Wenk, and D. J. Williams, "Texture measurements using the new neutron diffractometer HIPPO and their analysis using the Rietveld method," *Powder Diffraction*, vol. 19, no. 1, pp. 65–68, 2004.

[79] H. M. Reiche, S. C. Vogel, P. Mosbrucker, E. J. Larson, and M. R. Daymond, "A furnace with rotating load frame for in situ high temperature deformation and creep experiments in a neutron diffraction beam line," *Review of Scientific Instruments*, vol. 83, no. 5, Article ID 053901, 7 pages, 2012.

[80] H. M. Reiche and S. C. Vogel, "A versatile automated sample changer for texture measurements on the high pressure-preferred orientation neutron diffractometer," *Review of Scientific Instruments*, vol. 81, no. 9, Article ID 093302, 6 pages, 2010.

[81] D. Bhattacharyya, G. B. Viswanathan, S. C. Vogel, D. J. Williams, V. Venkatesh, and H. L. Fraser, "A study of the mechanism of α to β phase transformation by tracking texture evolution with temperature in Ti-6Al-4V using neutron diffraction," *Scripta Materialia*, vol. 54, no. 2, pp. 231–236, 2006.

[82] H. R. Wenk, I. Lonardelli, and D. Williams, "Texture changes in the hcp → bcc → hcp transformation of zirconium studied in

situ by neutron diffraction," *Acta Materialia*, vol. 52, no. 7, pp. 1899–1907, 2004.

[83] M. R. Daymond, R. A. Holt, S. Cai, P. Mosbrucker, and S. C. Vogel, "Texture inheritance and variant selection through an hcp-bcc-hcp phase transformation," *Acta Materialia*, vol. 58, no. 11, pp. 4053–4066, 2010.

[84] R. W. L. Fong, R. Miller, H. J. Saari, and S. C. Vogel, "Crystallographic texture and volume fraction of α and β phases in Zr-2.5Nb pressure tube material during heating and cooling," *Metallurgical and Materials Transactions A*, vol. 43, no. 3, pp. 806–821, 2012.

[85] E. Garlea, H. Choo, G. Y. Wang et al., "Hydride-phase formation and its influence on fatigue crack propagation behavior in a zircaloy-4 alloy," *Metallurgical and Materials Transactions A*, vol. 41, no. 11, pp. 2816–2828, 2010.

[86] P. J. Withers, M. Turski, L. Edwards, P. J. Bouchard, and D. J. Buttle, "Recent advances in residual stress measurement," *International Journal of Pressure Vessels and Piping*, vol. 85, no. 3, pp. 118–127, 2008.

[87] L. Edwards, P. J. Bouchard, M. Dutta et al., "Direct measurement of the residual stresses near a "boat-shaped" repair in a 20 mm thick stainless steel tube butt weld," *International Journal of Pressure Vessels and Piping*, vol. 82, no. 4, pp. 288–298, 2005.

[88] P. J. Bouchard, D. George, J. R. Santisteban et al., "Measurement of the residual stresses in a stainless steel pipe girth weld containing long and short repairs," *International Journal of Pressure Vessels and Piping*, vol. 82, no. 4, pp. 299–310, 2005.

[89] S. Paddea, J. A. Francis, A. M. Paradowska, P. J. Bouchard, and I. A. Shibli, "Residual stress distributions in a P91 steel-pipe girth weld before and after post weld heat treatment," *Materials Science and Engineering A*, vol. 534, pp. 663–672, 2012.

[90] D. G. Carr, M. I. Ripley, T. M. Holden, D. W. Brown, and S. C. Vogel, "Residual stress measurements in a zircaloy-4 weld by neutron diffraction," *Acta Materialia*, vol. 52, no. 14, pp. 4083–4091, 2004.

[91] D. G. Carr, M. I. Ripley, D. W. Brown, S. C. Vogel, and T. M. Holden, "Residual stress measurements on a stress relieved zircaloy-4 weld by neutron diffraction," *Journal of Nuclear Materials*, vol. 359, no. 3, pp. 202–207, 2006.

[92] D. Carr, T. Holden, M. Ripley, D. Brown, and S. Vogel, "Investigation of grain-scale stresses and modeling of tensile deformation in a zircaloy-4 weldment," *Metallurgical and Materials Transactions A*, vol. 38, no. 10, pp. 2410–2418, 2007.

[93] G. Ribárik, J. Gubicza, and T. Ungár, "Correlation between strength and microstructure of ball-milled Al–Mg alloys determined by X-ray diffraction," *Materials Science and Engineering A*, vol. 387-389, no. 1-2, pp. 343–347, 2004.

[94] L. Balogh, D. W. Brown, P. Mosbrucker, F. Long, and M. R. Daymond, "Dislocation structure evolution induced by irradiation and plastic deformation in the Zr-2.5 Nb nuclear structural material determined by neutron diffraction line profile analysis," *Acta Materialia*, vol. 60, no. 15, pp. 5567–5577, 2012.

[95] M. R. Daymond and P. J. Bouchard, "Elastoplastic deformation of 316 stainless steel under tensile loading at elevated temperatures," *Metallurgical and Materials Transactions A*, vol. 37, no. 6, pp. 1863–1873, 2006.

[96] B. Clausen, D. W. Brown, M. A. M. Bourke, T. A. Saleh, and S. A. Maloy, "In situ neutron diffraction and elastic-plastic self-consistent polycrystal modeling of HT-9," *Journal of Nuclear Materials*, vol. 425, no. 1–3, pp. 228–232, 2012.

[97] N. R. Barton, A. Arsenlis, and J. Marian, "A polycrystal plasticity model of strain localization in irradiated iron," *Journal of the Mechanics and Physics of Solids*, vol. 61, no. 2, pp. 341–351, 2013.

[98] K. E. Sickafus, L. Minervini, R. W. Grimes et al., "Radiation tolerance of complex oxides," *Science*, vol. 289, no. 5480, pp. 748–751, 2000.

[99] M. James, M. L. Carter, Z. Zhang et al., "Crystal chemistry and structures of (Ca,U) titanate pyrochlores," *Journal of the American Ceramic Society*, vol. 93, no. 10, pp. 3464–3473, 2010.

[100] T. Hartmann, A. Alaniz, F. Poineau et al., "Structure studies on lanthanide technetium pyrochlores as prospective host phases to immobilize ^{99}technetium and fission lanthanides from effluents of reprocessed used nuclear fuels," *Journal of Nuclear Materials*, vol. 411, no. 1–3, pp. 60–71, 2011.

[101] Y. Zhang, Z. Zhang, G. Thorogood, and E. Vance, "Pyrochlore based glass-ceramics for the immobilization of actiniderich nuclear wastes: from concept to reality," *Journal of Nuclear Materials*, vol. 432, no. 1–3, pp. 545–547, 2013.

[102] F. Izumi and K. Momma, "Three-dimensional visualization of electron- and nuclear-density distributions in inorganic materials by MEM-based technology," *IOP Conference Series: Materials Science and Engineering*, vol. 18, Article ID 022001, 2011.

[103] K. Momma and F. Izumi, "Evaluation of algorithms and weighting methods for mem analysis from powder diffraction data," *ZeitschriFt für Kristallographie Proceedings*, vol. 1, pp. 195–200, 2011.

[104] S. I. Nishimura, G. Kobayashi, K. Ohoyama, R. Kanno, M. Yashima, and A. Yamada, "Experimental visualization of lithium diffusion in Li_xFePO_4," *Nature Materials*, vol. 7, no. 9, pp. 707–711, 2008.

[105] J. Han, J. Zhu, Y. Li et al., "Experimental visualization of lithium conduction pathways in garnet-type $Li_7La_3Zr_2O_{12}$," *Chemical Communications*, vol. 48, no. 79, pp. 9840–9842, 2012.

[106] N. Takenaka, H. Asano, T. Fujii, M. Mizubata, and K. Yoshii, "Application of fast neutron radiography to three-dimensional visualization of steady two-phase flow in a rod bundle," *Nuclear Instruments and Methods in Physics Research A*, vol. 424, no. 1, pp. 73–76, 1999.

[107] R. Zboray, J. Kickhofel, M. Damsohn, and H. M. Prasser, "Cold-neutron tomography of annular flow and functional spacer performance in a model of a boiling water reactor fuel rod bundle," *Nuclear Engineering and Design*, vol. 241, no. 8, pp. 3201–3215, 2011.

[108] A. S. Tremsin, J. B. McPhate, J. V. Vallerga et al., "Detection efficiency, spatial and timing resolution of thermal and cold neutron counting MCP detectors," *Nuclear Instruments and Methods in Physics Research A*, vol. 604, no. 1-2, pp. 140–143, 2009.

[109] W. E. Lamb Jr., "Capture of neutrons by atoms in a crystal," *Physical Review*, vol. 55, no. 2, pp. 190–197, 1939.

[110] R. A. Schrack, J. W. Behrens, R. Johnson, and C. D. Bowman, "Resonance Neutron Radiography using an electron linac," *IEEE Transactions on Nuclear Science*, vol. NS-28, no. 2, pp. 1640–1164, 1980.

[111] G. Chen and R. C. Lanza, "Fast neutron resonance radiography for elemental imaging: theory and applications," *IEEE Transactions on Nuclear Science*, vol. 49, no. 4, pp. 1919–1924, 2002.

[112] H. Postma and P. Schillebeeckx, "Non-destructive analysis of objects using neutron resonance capture," *Journal of Radioanalytical and Nuclear Chemistry*, vol. 265, no. 2, pp. 297–302, 2005.

[113] H. Postma and P. Schillebeeckx, "Neutron resonance capture and transmission analysis," in *Encyclopedia of Analytical Chemistry*, 2009.

[114] D. L. Chichester and J. W. Sterbentz, "Neutron resonance transmission analysis (NRTA): initial studies of a method for assaying plutonium in spent fuel," Tech. Rep., Idaho National Laboratory (INL), 2011.

[115] D. L. Chichester and J. W. Sterbentz, *A Second Look at Neutron Resonance Transmission Analysis as a Spent Fuel NDA*, 2011.

[116] C. L. Morris, M. Bourke, D. D. Byler et al., "Qualitative comparison of bremsstrahlung X-rays and 800 MeV protons for tomography of urania fuel pellets," *Review of Scientific Instruments*, vol. 84, no. 2, Article ID 023902, 2013.

[117] A. Tremsin, S. Vogel, M. Mocko et al., "Non-destructive studies of fuel rodlets by neutron resonance absorption radiography and thermal neutron radiography," *Journal of Nuclear Materials*, 2013.

[118] M. B. Aufderheide III, H. S. Park, E. P. Hartouni et al., "Proton radiography as a means of material characterization," *AIP Conference Proceedings*, vol. 497, pp. 706–712, 1999.

[119] G. Burca, J. A. James, W. Kockelmann et al., "A new bridge technique for neutron tomography and diffraction measurements," *Nuclear Instruments and Methods in Physics Research A*, vol. 651, no. 1, pp. 229–235, 2011.

[120] W. Kockelmann, L. C. Chapon, and P. G. Radaelli, "Neutron texture analysis on GEM at ISIS," *Physica B*, vol. 385-386, pp. 639–643, 2006.

[121] A. Huq, J. P. Hodges, O. Gourdon, and L. Heroux, "Powgen: a third-generation highresolution high-throughput powder diffraction instrument at the spallation neutron source," *Zeitschrift für Kristallographie Proceedings*, vol. 1, pp. 127–135, 2011.

[122] T. Ishigaki, A. Hoshikawa, M. Yonemura et al., "IBARAKI materials design diffractometer (iMATERIA)—versatile neutron diffractometer at J-PARC," *Nuclear Instruments and Methods in Physics Research A*, vol. 600, no. 1, pp. 189–191, 2009.

[123] J. R. Santisteban, M. R. Daymond, J. A. James, and L. Edwards, "ENGIN-X: a third-generation neutron strain scanner," *Journal of Applied Crystallography*, vol. 39, no. 6, pp. 812–825, 2006.

[124] X. L. Wang, T. M. Holden, G. Q. Rennich et al., "VULCAN—the engineering diffractometer at the SNS," *Physica B*, vol. 385-386, pp. 673–675, 2006.

[125] S. Harjo, T. Ito, K. Aizawa et al., "Current status of engineering materials diffractometer at J-PARC," *Materials Science Forum*, vol. 681, pp. 443–448, 2011.

[126] O. Kirstein, V. Luzin, A. Brule, H. Nguyen, and D. Tawfik, "Kowari—OPAL's residual-stress diffractometer and its application to materials science and engineering," *Advanced Materials Research*, vol. 41-42, pp. 439–444, 2008.

[127] B. C. Larson, W. Yang, G. E. Ice, J. D. Budai, and J. Z. Tischler, "Three-dimensional X-ray structural microscopy with submicrometre resolution," *Nature*, vol. 415, no. 6874, pp. 887–890, 2002.

[128] J. D. Budai, W. Yang, N. Tamura et al., "X-ray microdiffraction study of growth modes and crystallographic tilts in oxide films on metal substrates," *Nature Materials*, vol. 2, no. 7, pp. 487–492, 2003.

[129] G. E. Ice, B. C. Larson, W. Yang et al., "Polychromatic X-ray microdiffraction studies of mesoscale structure and dynamics," *Journal of Synchrotron Radiation*, vol. 12, no. 2, pp. 155–162, 2005.

[130] J. Mayers, G. Baciocco, and A. C. Hannon, "Temperature measurement by neutron resonance radiography," *Nuclear Instruments and Methods in Physics Research A*, vol. 275, no. 2, pp. 453–459, 1989.

[131] J. C. Frost, P. Meehan, S. R. Morris, R. C. Ward, and J. Mayers, "Non-intrusive temperature measurement of the components of a working catalyst by neutron resonance radiography," *Catalysis Letters*, vol. 2, no. 2, pp. 97–104, 1989.

[132] Y. Le Godec, M. T. Dove, D. J. Francis et al., "Neutron diffraction at simultaneous high temperatures and pressures, with measurement of temperature by neutron radiography," *Mineralogical Magazine*, vol. 65, no. 6, pp. 737–748, 2001.

[133] H. J. Stone, M. G. Tucker, F. M. Meducin et al., "Temperature measurement in a Paris-Edinburgh cell by neutron resonance spectroscopy," *Journal of Applied Physics*, vol. 98, no. 6, Article ID 064905, 10 pages, 2005.

[134] H. J. Stone, M. G. Tucker, Y. Le Godec et al., "Remote determination of sample temperature by neutron resonance spectroscopy," *Nuclear Instruments and Methods in Physics Research A*, vol. 547, no. 2-3, pp. 601–615, 2005.

[135] V. W. Yuan, J. D. Bowman, D. J. Funk et al., "Shock temperature measurement using neutron resonance spectroscopy," *Physical Review Letters*, vol. 94, no. 12, Article ID 125504, 4 pages, 2005.

[136] D. C. Swift, A. Seifter, D. B. Holtkamp, V. W. Yuan, D. Bowman, and D. A. Clark, "Explanation of anomalous shock temperatures in shock-loaded Mo samples measured using neutron resonance spectroscopy," *Physical Review B*, vol. 77, no. 9, Article ID 092102, 4 pages, 2008.

[137] H. Sato, T. Kamiyama, and Y. Kiyanagi, "Pulsed neutron imaging using resonance transmission spectroscopy," *Nuclear Instruments and Methods in Physics Research A*, vol. 605, no. 1-2, pp. 36–39, 2009.

[138] M. Gu, H. Fang, B. Liu et al., "Indicator to estimate temperature sensitivity of resonance in temperature measurement by neutron resonance spectroscopy," *Nuclear Instruments and Methods in Physics Research B*, vol. 269, no. 5, pp. 528–538, 2011.

[139] H. Sato, T. Kamiyama, Y. Kiyanagi, and S. Ikeda, "Simulation for neutron resonance absorption spectroscopic tomography," *Nuclear Instruments and Methods in Physics Research A*, vol. 600, no. 1, pp. 135–138, 2009.

[140] T. Kamiyama, H. Sato, N. Miyamoto, H. Iwasa, Y. Kiyanagi, and S. Ikeda, "Energy sliced neutron tomography using neutron resonance absorption spectrometer," *Nuclear Instruments and Methods in Physics Research A*, vol. 600, no. 1, pp. 107–110, 2009.

[141] A. S. Tremsin, J. B. McPhate, J. V. Vallerga et al., "High resolution neutron resonance absorption imaging at a pulsed neutron beamline," in *Proceedings of the IEEE Nuclear Science Symposium and Medical Imaging Conference (NSS/MIC '11)*, pp. 1501–1505, IEEE, October 2011.

[142] A. Tremsin, J. McPhate, J. Vallerga et al., "Spatially resolved remote measurement of temperature by neutron resonance absorption," in *Proceedings of the IEEE Nuclear Science Symposium*, IEEE, Los Angeles, Calif, USA, October 2012.

[143] E. M. Schooneveld, M. Tardocchi, G. Gorini et al., "A new position-sensitive transmission detector for epithermal neutron imaging," *Journal of Physics D*, vol. 42, no. 15, Article ID 152003, 2009.

[144] X. Llopart, R. Ballabriga, M. Campbell, L. Tlustos, and W. Wong, "Timepix, a 65k programmable pixel readout chip for arrival time, energy and/or photon counting measurements," *Nuclear Instruments and Methods in Physics Research A*, vol. 581, no. 1-2, pp. 485–494, 2007.

[145] A. S. Tremsin, W. B. Feller, and R. G. Downing, "Efficiency optimization of microchannel plate (MCP) neutron imaging detectors. I. Square channels with ^{10}B doping," *Nuclear Instruments and Methods in Physics Research A*, vol. 539, no. 1-2, pp. 278–311, 2005.

[146] A. S. Tremsin, J. B. McPhate, J. V. Vallerga et al., "Improved efficiency of high resolution thermal and cold neutron imaging," *Nuclear Instruments and Methods in Physics Research A*, vol. 628, no. 1, pp. 415–418, 2011.

[147] K. Meggers, H. G. Priesmeyer, M. Stalder, S. Vogel, and W. Trela, "Single-shot neutron transmission diffraction," *Physica B*, vol. 234–236, pp. 1160–1162, 1997.

[148] S. Vogel, *A Rietveld-Approach for the Analysis of Neutron Time-of-Flight Transmission Data*, Mathematisch-Naturwissenschaftliche Fakultät, University of Kiel, Kiel, Germany, 2000.

[149] J. R. Santisteban, L. Edwards, M. E. Fizpatrick, A. Steuwer, and P. J. Withers, "Engineering applications of Bragg-edge neutron transmission," *Applied Physics A*, vol. 74, no. 1, supplement, pp. s1433–s1436, 2002.

[150] J. R. Santisteban, L. Edwards, H. G. Priesmeyer, and S. Vogel, "Comparison of Bragg-edge neutron-transmission spectroscopy at ISIS and LANSCE," *Applied Physics A*, vol. 74, no. 1, supplement, pp. s1616–s1618, 2002.

[151] J. Huang, S. C. Vogel, W. J. Poole, M. Militzer, and P. Jacques, "The study of low-temperature austenite decomposition in a Fe–C–Mn–Si steel using the neutron Bragg edge transmission technique," *Acta Materialia*, vol. 55, no. 8, pp. 2683–2693, 2007.

[152] H. Sato, T. Kamiyama, and Y. Kiyanagi, "A Rietveld-type analysis code for pulsed neutron Bragg-edge transmission imaging and quantitative evaluation of texture and microstructure of a welded α-iron plate," *Materials Transactions*, vol. 52, no. 6, pp. 1294–1302, 2011.

[153] A. S. Tremsin, J. B. McPhate, J. V. Vallerga et al., "Transmission Bragg edge spectroscopy measurements at ORNL spallation neutron source," *Journal of Physics: Conference Series*, vol. 251, no. 1, Article ID 012069, 2010.

[154] A. S. Tremsin, J. B. McPhate, W. Kockelmann, J. V. Vallerga, O. H. W. Siegmund, and W. B. Feller, "High resolution Bragg edge transmission spectroscopy at pulsed neutron sources: proof of principle experiments with a neutron counting MCP detector," *Nuclear Instruments and Methods in Physics Research A*, vol. 633, supplement 1, pp. S235–S238, 2011.

[155] A. S. Tremsin, J. B. Mcphate, A. Steuwer et al., "High-resolution strain mapping through time-of-flight neutron transmission diffraction with a microchannel plate neutron counting detector," *Strain*, vol. 48, no. 4, pp. 296–305, 2012.

[156] S. Vogel, E. Ustundag, J. C. Hanan, V. W. Yuan, and M. A. M. Bourke, "In-situ investigation of the reduction of NiO by a neutron transmission method," *Materials Science and Engineering A*, vol. 333, no. 1-2, pp. 1–9, 2002.

[157] A. Steuwer, P. J. Withers, J. R. Santisteban, and L. Edwards, "Using pulsed neutron transmission for crystalline phase imaging and analysis," *Journal of Applied Physics*, vol. 97, no. 7, Article ID 074903, 2005.

[158] E. H. Lehmann, P. Vontobel, and A. Hermann, "Non-destructive analysis of nuclear fuel by means of thermal and cold neutrons," *Nuclear Instruments and Methods in Physics Research A*, vol. 515, no. 3, pp. 745–759, 2003.

[159] F. Groeschel, P. Schleuniger, A. Hermann, E. Lehmann, and L. Wiezel, "Neutron radiography of irradiated fuel rod segments at the SINQ: loading, transfer and irradiation concept," *Nuclear Instruments and Methods in Physics Research A*, vol. 424, no. 1, pp. 215–220, 1999.

[160] E. Lehmann, P. Vontobel, and M. Estermann, "Study of material changes of SINQ target rods after long-term exposure by neutron radiography methods," *Applied Radiation and Isotopes*, vol. 61, no. 4, pp. 603–607, 2004.

[161] P. Vontobel, M. Tamaki, N. Mori et al., "Post-irradiation analysis of SINQ target rods by thermal neutron radiography," *Journal of Nuclear Materials*, vol. 356, no. 1–3, pp. 162–167, 2006.

[162] M. Grosse, M. Steinbrueck, E. Lehmann, and P. Vontobel, "Kinetics of hydrogen absorption and release in zirconium alloys during steam oxidation," *Oxidation of Metals*, vol. 70, no. 3-4, pp. 149–162, 2008.

[163] E. H. Lehmann, P. Vontobel, and N. Kardjilov, "Hydrogen distribution measurements by neutrons," *Applied Radiation and Isotopes*, vol. 61, no. 4, pp. 503–509, 2004.

[164] R. Yasuda, M. Nakata, M. Matsubayashi, K. Harada, Y. Hatakeyama, and H. Amano, "Application of hydrogen analysis by neutron imaging plate method to zircaloy cladding tubes," *Journal of Nuclear Materials*, vol. 320, no. 3, pp. 223–230, 2003.

[165] E. Sváb, G. Mészáros, Z. Somogyvári, M. Balaskó, and F. Körösi, "Neutron imaging of Zr-1% Nb fuel cladding material containing hydrogen," *Applied Radiation and Isotopes*, vol. 61, no. 4, pp. 471–477, 2004.

[166] A. Shaikh, P. Vaidya, B. Shah, S. Gangotra, and K. Sahoo, "Application of neutron radiography and neutron diffraction techniques in study of zirconium hydride blisters in zirconium based pressure tube materials," *BARC Newsletter*, vol. 273, p. 104, 2006.

[167] M. Grosse, G. Kuehne, M. Steinbrueck, E. Lehmann, J. Stuckert, and P. Vontobel, "Quantification of hydrogen uptake of steam-oxidized zirconium alloys by means of neutron radiography," *Journal of Physics Condensed Matter*, vol. 20, no. 10, Article ID 104263, 2008.

[168] M. Grosse, M. Steinbrueck, and A. Kaestner, "Wavelength dependent neutron transmission and radiography investigations of the high temperature behaviour of materials applied in nuclear fuel and control rod claddings," *Nuclear Instruments and Methods in Physics Research A*, vol. 651, no. 1, pp. 315–319, 2011.

[169] M. Große, M. Steinbrück, J. Stuckert, A. Kastner, and B. Schillinger, "Application of neutron radiography to study material processes during hypothetical severe accidents in nuclear reactors," *Journal of Materials Science*, vol. 47, no. 18, pp. 6505–6512, 2012.

[170] J. R. Granada, J. R. Santisteban, and R. E. Mayer, "Non-destructive determination of very low hydrogen content in metals with the use of neutron techniques," *Physica B*, vol. 213-214, pp. 1005–1007, 1995.

[171] L. Bennun, J. Santisteban, J. Díaz-Valdés, J. R. Granada, and R. E. Mayer, "A neutronic method to determine low hydrogen concentrations in metals," *Nuclear Instruments and Methods in Physics Research B*, vol. 263, no. 2, pp. 468–472, 2007.

[172] Y. N. Choi, H. S. Oh, V. T. Em, V. A. Somenkov, C. H. Lee, and S. D. Park, "Measurement of very small hydrogen content in zirconium alloys by measuring thermal neutron incoherent scattering," *Applied Physics A*, vol. 74, no. 1, supplement, pp. s1710–s1712, 2002.

[173] A. Couet, A. T. Motta, R. J. Comstock, and R. L. Paul, "Cold neutron prompt gamma activation analysis, a non-destructive technique for hydrogen level assessment in zirconium alloys," *Journal of Nuclear Materials*, vol. 425, no. 1–3, pp. 211–217, 2012.

[174] J. R. Santisteban, M. A. Vicente-Alvarez, P. Vizcaino et al., "Texture imaging of zirconium based components by total neutron cross-section experiments," *Journal of Nuclear Materials*, vol. 425, no. 1–3, pp. 218–227, 2012.

[175] M. Strobl, "Future prospects of imaging at spallation neutron sources," *Nuclear Instruments and Methods in Physics Research A*, vol. 604, no. 3, pp. 646–652, 2009.

[176] G. E. Ice, C. R. Hubbard, B. C. Larson et al., "Kirkpatrick-Baez microfocusing optics for thermal neutrons," *Nuclear Instruments and Methods in Physics Research A*, vol. 539, no. 1-2, pp. 312–320, 2005.

[177] G. E. Ice, C. R. Hubbard, B. C. Larson et al., "High-performance Kirkpatrick-Baez supermirrors for neutron milli- and microbeams," *Materials Science and Engineering A*, vol. 437, no. 1, pp. 120–125, 2006.

[178] S. J. Kisner, E. Haneda, C. A. Bouman, S. Skatter, M. Kourinny, and S. Bedford, "Limited view angle iterative CT reconstruction," in *10th Computational Imaging*, vol. 8296 of *Proceedings of SPIE*, p. 7, Burlingame, Calif, USA, January 2012.

[179] R. Zhang, A. Chang, J. B. Thibault, K. Sauer, and C. Bouman, "Statistical modeling challenges in model-based reconstruction for x-ray CT," in *11th Computational Imaging*, vol. 8657 of *Proceedings of SPIE*, Burlingame, Calif, USA, February 2013.

[180] J. Wang, K. Sauer, J. B. Thibault, Z. Yu, and C. Bouman, "Prediction coefficient estimation in markov random fields for iterative x-ray ct reconstruction," in *Medical Imaging 2012: Image Processing*, vol. 8314 of *Proceedings of SPIE*, p. 831444, San Diego, Calif, USA, February 2012.

[181] G. Chaboussant, S. Désert, and A. Brûlet, "Recent developments and projects in SANS instrumentation at LLB-Orphée," *The European Physical Journal Special Topics*, vol. 213, no. 1, pp. 313–325, 2012.

[182] M. H. Mathon, Y. de Carlan, G. Geoffroy, X. Averty, A. Alamo, and C. H. De Novion, "A SANS investigation of the irradiation-enhanced α-α' phases separation in 7–12 Cr martensitic steels," *Journal of Nuclear Materials*, vol. 312, no. 2-3, pp. 236–248, 2003.

[183] M. J. Alinger, G. R. Odette, and D. T. Hoelzer, "The development and stability of Y–Ti–O nanoclusters in mechanically alloyed Fe–Cr based ferritic alloys," *Journal of Nuclear Materials*, vol. 329–333, pp. 382–386, 2004.

[184] P. J. Bouchard, P. J. Withers, S. A. McDonald, and R. K. Heenan, "Quantification of creep cavitation damage around a crack in a stainless steel pressure vessel," *Acta Materialia*, vol. 52, no. 1, pp. 23–34, 2004.

[185] O. Anderoglu, J. Van den Bosch, P. Hosemann et al., "Phase stability of an HT-9 duct irradiated in FFTF," *Journal of Nuclear Materials*, vol. 430, no. 1–3, pp. 194–204, 2012.

[186] P. Seeger, R. Hjelm Jr., and M. Nutter, "The low-Q diffractometer at the Los Alamos neutron scattering center," *Molecular Crystals and Liquid Crystals*, vol. 180, pp. 101–117, 1990.

[187] C. D. Bowman, D. C. Bowman, T. Hill et al., "Measurements of thermal neutron diffraction and inelastic scattering in reactor-grade graphite," *Nuclear Science and Engineering*, vol. 159, no. 2, pp. 182–198, 2008.

[188] J. E. Lynn, G. H. Kwei, W. J. Trela et al., "Vibrational properties of Pu and Ga in a Pu–Ga alloy from neutron-resonance Doppler spectroscopy," *Physical Review B*, vol. 58, no. 17, pp. 11408–11415, 1998.

[189] N. J. Lane, S. C. Vogel, G. Hug et al., "Neutron diffraction measurements and first-principles study of thermal motion of atoms in select $M_{n+1}AX_n$ and binary MX transition-metal carbide phases," *Physical Review B*, vol. 86, no. 21, Article ID 214301, 9 pages, 2012.

[190] K. Clausen, W. Hayes, J. E. MacDonald, R. Osborn, and M. T. Hutchings, "Observation of oxygen Frenkel disorder in uranium dioxide above 2000 K by use of neutron-scattering techniques," *Physical Review Letters*, vol. 52, no. 14, pp. 1238–1241, 1984.

[191] K. N. Clausen, M. A. Hackett, W. Hayes et al., "Coherent diffuse neutron scattering from UO_2 and ThO_2 at temperatures above 2000 K," *Physica B*, vol. 156-157, pp. 103–106, 1989.

[192] J. P. Goff, B. Fåk, W. Hayes, and M. T. Hutchings, "Defect structure and oxygen diffusion in UO_2+δ," *Journal of Nuclear Materials*, vol. 188, pp. 210–215, 1992.

[193] K. Clausen, W. Hayes, M. Hutchings, J. Macdonald, R. Osborn, and P. Schnabel, "Investigation of oxygen disorder, thermal parameters, lattice vibrations and elastic constants of UO_2 and ThO_2 at temperatures up to 2 930 K," *Revue de Physique Appliquée*, vol. 19, pp. 719–722, 1984.

[194] M. T. Hutchings, "High-temperature studies of UO_2 and ThO_2 using neutron scattering techniques," *Journal of the Chemical Society, Faraday Transactions 2*, vol. 83, no. 7, pp. 1083–1103, 1987.

[195] T. Proffen, S. J. L. Billinge, T. Egami, and D. Louca, "Structural analysis of complex materials using the atomic pair distribution function—a practical guide," *Zeitschrift für Kristallographie*, vol. 218, no. 2, pp. 132–143, 2003.

[196] A. C. Wright, B. Bachra, T. M. Brunier, R. N. Sinclair, L. F. Gladden, and R. L. Portsmouth, "A neutron diffraction and MAS-NMR study of the structure of fast neutron irradiated vitreous silica," *Journal of Non-Crystalline Solids*, vol. 150, no. 1–3, pp. 69–75, 1992.

[197] F. Garrido, A. C. Hannon, R. M. Ibberson, L. Nowicki, and B. T. M. Willis, "Neutron diffraction studies of U_4O_9: comparison with EXAFS results," *Inorganic Chemistry*, vol. 45, no. 20, pp. 8408–8413, 2006.

[198] S. D. Conradson, D. Manara, F. Wastin et al., "Local structure and charge distribution in the UO_2-U_4O_9 system," *Inorganic Chemistry*, vol. 43, no. 22, pp. 6922–6935, 2004.

[199] L. Desgranges, G. Baldinozzi, D. Siméone, and H. E. Fischer, "Refinement of the α-U_4O_9 crystalline structure: new insight into the $U_4O_9 \rightarrow U_3O_8$ transformation," *Inorganic Chemistry*, vol. 50, no. 13, pp. 6146–6151, 2011.

[200] G. Dolling, R. Cowley, and A. Woods, "The crystal dynamics of uranium dioxide," *Canadian Journal of Physics*, vol. 43, no. 8, pp. 1397–1413, 1965.

[201] R. J. McQueeney, A. C. Lawson, A. Migliori et al., "Unusual phonon softening in δ-phase plutonium," *Physical Review Letters*, vol. 92, no. 14, Article ID 146401, 4 pages, 2004.

[202] M. Dubey, M. S. Jablin, P. Wang, M. Mocko, and J. Majewski, "SPEAR-ToF neutron reflectometer at the Los Alamos neutron science center," *European Physical Journal Plus*, vol. 126, no. 11, pp. 1–11, 2011.

[203] H. He, P. Wang, D. Allred, J. Majewski, M. Wilkerson, and K. D. Rector, "Characterization of chemical speciation in ultrathin uranium oxide layered films," *Analytical Chemistry*, vol. 84, no. 23, pp. 10380–10387, 2012.

[204] A. C. Larson and R. B. Von Dreele, "General structure analysis system (GSAS)," Tech. Rep. LA-UR 86-748, Los Alamos National Laboratory (LANL), 2004.

[205] S. C. Vogel, "Gsaslanguage: a GSAS script language for automated Rietveld refinements of diffraction data," *Journal of Applied Crystallography*, vol. 44, no. 4, pp. 873–877, 2011.

[206] K. Momma and F. Izumi, "VESTA 3 for three-dimensional visualization of crystal, volumetric and morphology data," *Journal of Applied Crystallography*, vol. 44, no. 6, pp. 1272–1276, 2011.

[207] H. M. Reiche, *Advanced sample environments for in situ neutron diffraction studies of nuclear materials [Ph.D. thesis]*, New Mexico State University, Las Cruces, NM, USA, 2012.

[208] S. Matthies, J. Pehl, H. R. Wenk, L. Lutterotti, and S. C. Vogel, "Quantitative texture analysis with the HIPPO neutron TOF diffractometer," *Journal of Applied Crystallography*, vol. 38, no. 3, pp. 462–475, 2005.

[209] H. R. Wenk, L. Lutterotti, and S. C. Vogel, "Rietveld texture analysis from TOF neutron diffraction data," *Powder Diffraction*, vol. 25, no. 3, Article ID 008003PDJ, pp. 283–296, 2010.

[210] A. Kahle, B. Winkler, B. Hennion, and P. Boutrouille, "High-temperature furnace for dynamic neutron radiography," *Review of Scientific Instruments*, vol. 74, no. 8, pp. 3717–3721, 2003.

[211] A. Kahle, B. Winkler, and B. Hennion, "Is Faxén's correction function applicable to viscosity measurements of silicate melts with the falling sphere method?" *Journal of Non-Newtonian Fluid Mechanics*, vol. 112, no. 2-3, pp. 203–215, 2003.

[212] B. Winkler, A. Kahle, and B. Hennion, "Neutron radiography of rocks and melts," *Physica B*, vol. 385-386, pp. 933–934, 2006.

[213] C. W. Barnes, M. Bourke, S. Malloy et al., "Radiation damage from atomic to meso-scales in extreme environments," *Bulletin of the American Physical Society*, vol. 55, 2010.

[214] "Experimental Physical Sciences VISTA: MaRIE," 2010, http://www.lanl.gov/orgs/adeps/VISTAS/docs/FINAL-LALP-10-059-reduced.pdf.

[215] "Matter-Radiation Interactions in Extremes (MaRIE), Los Alamos Lab," 2012, http://marie.lanl.gov/.